nature neuroscience

Article

https://doi.org/10.1038/s41593-024-01771-8

The hippocampal CA2 region discriminates social threat from social safety

Received: 27 July 2023

Accepted: 23 August 2024

Published online: 15 October 2024

Check for updates

Pegah Kassraian[1] ✉, Shivani K. Bigler[1], Diana M. Gilly Suarez[1], Neilesh Shrotri[1], Anastasia Barnett[1], Heon-Jin Lee[2,6], W. Scott Young[2] & Steven A. Siegelbaum[1,3,4,5]

The dorsal cornu ammonis 2 (dCA2) region of the hippocampus enables the discrimination of novel from familiar conspecifics. However, the neural bases for more complex social–spatial episodic memories are unknown. Here we report that the spatial and social contents of an aversive social experience require distinct hippocampal regions. While dorsal CA1 (dCA1) pyramidal neurons mediate the memory of an aversive location, dCA2 pyramidal neurons enable the discrimination of threat-associated (CS^+) from safety-associated (CS^-) conspecifics in both female and male mice. Silencing dCA2 during encoding or recall trials disrupted social fear discrimination memory, resulting in fear responses toward both the CS^+ and CS^- mice. Calcium imaging revealed that the aversive experience strengthened and stabilized dCA2 representations of both the CS^+ and CS^- mice, with the incorporation of an abstract representation of social valence into representations of social identity. Thus, dCA2 contributes to both social novelty detection and the adaptive discrimination of threat-associated from safety-associated individuals during an aversive social episodic experience.

Social memory, the recollection of encounters with conspecifics, is important for enabling an individual to recognize conspecifics based on the valence of past social interactions. An inability to distinguish individuals based on whether a past interaction was aversive or rewarding may lead to social withdrawal and social avoidance, hallmarks of social anxiety disorder[1,2] and post-traumatic stress disorder[3]. In humans, the hippocampus has been known to be critical for social memory since the pioneering studies of Brenda Milner and colleagues[4,5] on patient H.M. Studies on social memory in rodents have confirmed the role of the hippocampus in the encoding and recall of social memory[6], with the dorsal cornu ammonis 2 (dCA2) region found to be of particular importance[7–10], along with ventral CA1 (vCA1)[11,12], ventral CA3 (refs. 13,14) and the connections from dCA2 to vCA1 (refs. 11,14).

To date, studies of social memory in rodents have focused largely on social novelty recognition memory, which enables an animal to discriminate a novel from a familiar conspecific. However, similar to other forms of memory, social memory consists of two distinct cognitive components—the recognition of whether an individual is novel or familiar and the recollection of the details of previous social experiences, or episodes, with a familiar individual, including the valence of the encounter and its spatial location[15,16]. At present, the neural mechanisms that contribute to more complex forms of social memory, including the memory of the valence of a given social encounter that enables the discrimination of a threat-associated conspecific from a safety-associated conspecific, which we term social fear discrimination memory, remain unknown.

Despite the emerging evidence for the role of dCA2 in social novelty recognition memory, it is uncertain as to whether dCA2 is required for the recollection of more complex social memories that include the context, location and valence of past social encounters.

[1]Zuckerman Mind Brain Behavior Institute, Columbia University, New York City, NY, USA. [2]National Institute of Mental Health, National Institutes of Health, Bethesda, MD, USA. [3]Department of Neuroscience, Vagelos College of Physicians and Surgeons, Columbia University Irving Medical Center, New York City, NY, USA. [4]Department of Pharmacology, Vagelos College of Physicians and Surgeons, Columbia University Irving Medical Center, New York City, NY, USA. [5]Kavli Institute for Brain Science, Columbia University, New York City, NY, USA. [6]Present address: Department of Microbiology and Immunology, School of Dentistry, Kyungpook National University, Daegu, South Korea. ✉e-mail: pegahkf@gmail.com

Such social episodic memories likely require the participation of hippocampal regions outside the core dCA2 to vCA1 social novelty recognition memory circuit, including dorsal CA1 (dCA1), given its importance in the encoding of spatial and contextual information. Although dCA1 is not required for social novelty recognition memory[11,17], it does form social place cells that track the location of a conspecific[17–19]. However, at present, it is unclear as to whether dCA1 participates in social episodic memory and how it might interact with dCA2 to disentangle social and spatial information required for social fear discrimination memory.

Here we have developed a modified version of a standard social fear conditioning (SFC) protocol[20] that enabled us to examine the neural bases underlying the encoding of an aversive social–spatial episode in which a subject learned to discriminate a threat-associated from safety-associated conspecific and a threat-associated from safety-associated spatial location. In the standard SFC paradigm, an animal receives a foot shock when it approaches a conspecific. When tested on subsequent days, the subject will avoid a novel conspecific, similar to the social avoidance observed following an episode of social defeat[21–23]. A number of brain regions contribute to social fear and avoidance behaviors as a consequence of SFC, such as the prefrontal cortex[24], lateral septum[25,26], amygdala and ventral hippocampus[27], and as a consequence of the related paradigm of social defeat[21,22], including the ventrolateral subdivision of the ventromedial hypothalamus (VMHvl)[28,29]. However, previous paradigms used in both SFC and social defeat have not, in general, been optimized to allow the study of how an animal learns to distinguish a threatening social or spatial cue from nonthreatening cues it has previously encountered, limiting our understanding of the neural bases of social fear discrimination memory.

Results

To examine the neural mechanisms that enable an individual to discriminate threatening from nonthreatening spatial and social cues, we first used a modified social-spatial fear conditioning (SSFC) protocol in which a subject mouse explored a fear conditioning chamber containing two novel stimulus mice confined to wire cup cages at opposite ends of the chamber. The subject received a mild foot shock when it explored one stimulus mouse (CS^+) but not the other (CS^-) during a 5-min learning trial (Fig. 1a). After 24 h, we performed successive 5-min spatial and social recall trials. We first probed, in a spatial recall trial, the spatial specificity of fear memory by re-exposing the subject to the SFC chamber containing two empty cup cages in the same location as in the SFC session. Immediately afterward, we examined the social specificity of fear memory in two successive trials. We first performed a cup recall trial with the two empty cup cages placed at opposite ends of a novel arena to determine the saliency of these objects to fear memory behaviors. This was immediately followed by a social recall trial in the same novel arena with the CS^+ and CS^- mice inside the cups to examine the saliency of the social cues.

The SSFC protocol produced robust spatial avoidance memory and selective social fear discrimination memory during the respective spatial and social recall sessions in both male and female mice (Fig. 1b–h). During the spatial recall trial, the subjects spent a significantly greater fraction of time in the 'safe' arena half compared to the half in which they were shocked (Fig. 1d,e). Similarly, during the social recall trial, the subjects spent a significantly greater fraction of time in the half of the novel arena containing the CS^- mouse compared to the half containing the CS^+ mouse (Fig. 1d,g). The subjects also showed a marked increase in freezing after SSFC in both spatial (Fig. 1f) and social (Fig. 1h) recall trials, suggestive of a fear memory response. In contrast, the subjects showed little freezing in the cup recall trial in the novel arena, where there was neither spatial nor social information from the SFC trial (Fig. 1h), indicating the saliency of the spatial and social cues.

To what extent are the spatial and social components of SSFC memory localized to distinct hippocampal regions? Because of the importance of dCA1 pyramidal neurons in spatial memory[30,31] and of dCA2 pyramidal neurons in social novelty recognition memory[7–10,32], we addressed their roles by injecting Cre-dependent adeno-associated virus (AAV) to express the inhibitory hM4Di receptor (iDREADD) in dCA1 pyramidal neurons or dCA2 pyramidal neurons of female and male *Lypd1-Cre*$^+$ mice[17] or *Amigo2-Cre*$^+$ mice[7], respectively. In these experiments, Cre^+ littermate control animals were injected with Cre-dependent AAV to express mCherry. Approximately 3–4 weeks after viral injection, iDREADD-expressing Cre^+ mice and a balanced number of controls were intraperitoneally administered the iDREADD agonist clozapine-N-oxide (CNO; 5 mg kg^{-1}) 30 min before SSFC. We then tested social–spatial fear recall 24 h later in the absence of CNO (Fig. 1b–h).

Silencing dCA1 and dCA2 during the SSFC learning trial produced remarkably specific and complementary impairments in spatial and social memory components of SSFC, respectively, relative to the control groups. Thus, while the dCA1-silenced mice no longer discriminated between the foot shock-associated and safety-associated arena locations during the spatial recall trial, these mice maintained their normal avoidance of the CS^+ and preference for the CS^- mouse in the social recall trial (Fig. 1d,e,g). In contrast, dCA2-silenced mice maintained a normal preference for the safety-associated location in the spatial recall test but failed to discriminate between the CS^+ and the CS^- mice during the social recall trial. Thus, with dCA2 silenced, subjects spent comparable amounts of time in the CS^- and CS^+ halves of the recall arena, with most time spent in the arena center (Fig. 1d,e,g). Of particular interest, both dCA1- and dCA2-silenced mice continued to show increased freezing in both the spatial and social recall tests (Fig. 1f,h), indicating that, in both cases, the mice recalled the aversive experience of SSFC but could no longer discriminate safety-associated from threat-associated spatial locales or social stimuli. Of further interest, the subject mice showed no fear behavior during the empty cups session in the social recall arena, indicating that the fear response remained specific to a social context, even when dCA2 or dCA1 were silenced. Thus, neither dCA1 nor dCA2 were needed to encode a generalized threat; rather, they ensured the proper association of a threatening experience with the correct spatial or social cue.

Silencing dCA2 gives rise to generalized social avoidance

Given extensive previous studies of the role of dCA1 in spatial memory coding behaviors[30,31], we focused on the role of dCA2 in social fear discrimination memory using a simpler recall protocol that omitted the spatial recall test (Fig. 2a). We added a control group of mock-SFC mice that underwent the SFC protocol but did not receive foot shocks to control for repeated exposure of the subject to the stimulus mice. In addition, we used either *Amigo2-Cre* transgenic or *Avpr1b-Cre* knock-in mice[33] to achieve dCA2-selective targeting to provide additional controls for potential nonspecific effects of transgene insertion or gene knock-in. We used a supervised classification approach to characterize in more detail the behavior of subject mice and, in particular, their approach-avoidance behavior (Extended Data Fig. 1). As seen above, SFC in this protocol produced robust social fear behaviors and social fear discrimination in a 24 h recall test in both males and females, with increased freezing in the social but not empty cup recall session and increased time spent in the CS^- versus CS^+ halves of the arena (Extended Data Fig. 2a). In contrast, the subject mice showed no increased freezing and no difference in CS^+/CS^- arena half residence times following mock-SFC. We also found that SFC, but not mock-SFC, produced a robust social fear discrimination measured by differences in CS^+/CS^- interaction times (Fig. 2b), with a greater number of approach-avoidance events[24] towards the CS^+ as to the CS^- mouse (Fig. 2a,c–f). The social fear behavior in the SFC group was not associated with an increased general anxiety relative to the mock-SFC group as measured by the similar behaviors of the two groups in the elevated plus maze or in locomotor activity (Extended Data Fig. 3a,b).

We next examined the effect of chemogenetic silencing of dCA2 during the SFC learning trial on CS^+/CS^- interaction times and

https://doi.org/10.1038/s41593-024-01771-8

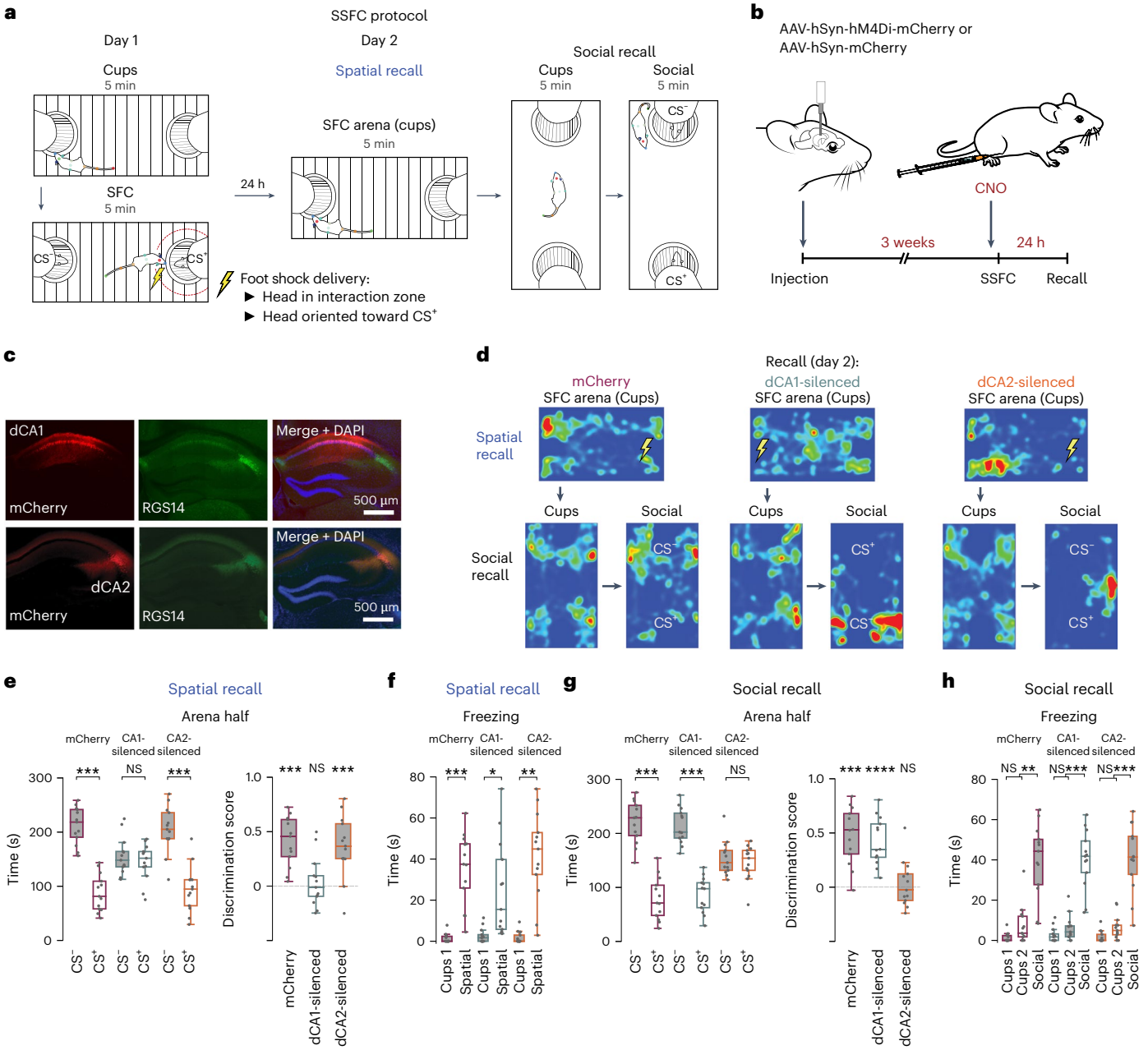

Fig. 1 | Differential roles for dCA2 and dCA1 in spatial and social aspects of social episodic memory. a, SSFC paradigm. Colored dots show pose estimation markers. **b**, Experimental timeline. **c**, Top row, coronal section showing hM4Di-mCherry in dCA1 pyramidal neurons from an *Lypd1-Cre* mouse. Bottom row, coronal section showing co-expression of hM4Di-mCherry and CA2 marker RGS14 in dCA2 pyramidal neurons from an *Amigo2-Cre* mouse. **d**, Example mouse position heatmaps during SSFC spatial (top panels) and social (bottom panels) recall sessions for mice expressing: left, mCherry in dCA1 (control); middle, hM4Di-mCherry in dCA1; and right, hM4Di-mCherry in dCA2. **e**–**h**, $n = 13$ *Lypd1-Cre*$^+$ (mCherry in dCA1), $n = 13$ *Lypd1-Cre*$^+$ (hM4Di-mCherry in dCA1), $n = 13$ *Amigo2-Cre*$^+$ (hm4Di-mCherry in dCA2). **e**, Left, mCherry and dCA2-silenced mice but not dCA1-silenced mice spent during spatial recall more time in chamber half where the CS$^-$ mouse was present in the SSFC learning trial (two-way repeated measures ANOVA—cohort × arena half, $F(2,72) = 17.7$, $P = 5.8 \times 10^{-7}$). Right, discrimination scores (Methods), two-tailed one-sample *t*-tests against zero. **f**, Time spent freezing during spatial recall (day 2) was significantly greater than that during the 'Cups' trial before SFC (day 1) for all three groups (two-way repeated measures ANOVA—cohort × stage, $F(2,72) = 4.34$, $P = 0.017$). **g**, Left, mCherry and dCA1-silenced mice but not CA2-silenced mice spent more time during social recall interacting with the CS$^-$ compared to CS$^+$ mouse during the social recall in the novel arena (two-way repeated measures ANOVA—cohort × arena half, $F(2,72) = 28.45$, $P = 7.8 \times 10^{-10}$). Right, discrimination scores, two-tailed one-sample *t*-tests against zero. **h**, Cohorts displayed similarly elevated freezing durations during social recall versus either Cups trial before SSFC (Cups 1) or cup recall trial after SSFC (Cups 2; three-way repeated measures ANOVA—Cups (Cups 1 or Cups 2) × social recall × cohort, $F(3,108) = 8.124$, $P = 0.014$). Box plots—central line, median; bottom and top edges, 25th and 75th percentiles; whiskers, most extreme data points (excluding outliers); dots, individual animals. Bonferroni post hoc and *t*-tests, as appropriate—*$P < 0.5$, **$P < 0.01$ and ***$P < 0.001$. Sex was balanced per condition, no sex differences were observed (for statistical comparison between females and males, see Supplementary Table 1). NS, not significant.

https://doi.org/10.1038/s41593-024-01771-8

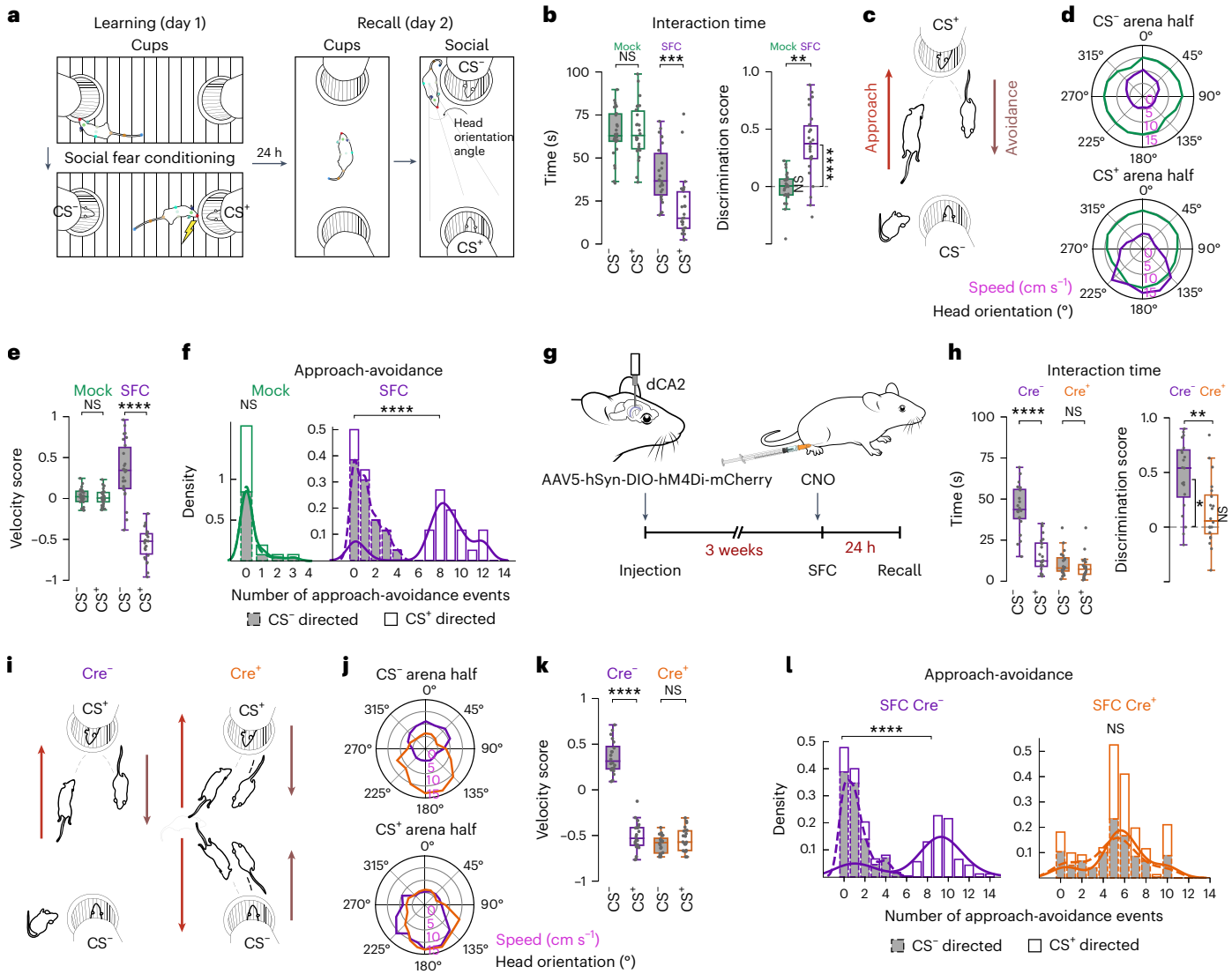

Fig. 2 | Social fear conditioning induces robust social fear discrimination memory that requires the activity of dCA2. **a**, SFC paradigm. **b**, Left, CS⁻ and CS⁺ interaction times after mock-SFC or SFC (two-way repeated measures ANOVA—cohort × stimulus mouse, $F(1,100) = 10.91$, $P = 1.32 \times 10^{-3}$). Right, discrimination scores. **b**–**f**, $n = 26$ C57BL/6J wild-type mice per cohort. Discrimination scores for **b** and **h**—unpaired, two-sided *t*-tests between cohorts; two-sided one-sample *t*-tests against zero. **c**, Illustration of approach-avoidance behaviors. **d**, Velocity versus head orientation angle plots toward CS⁻ (top) and CS⁺ (bottom) for mock-SFC (green) and SFC (purple) groups. Approach, 0° and retreat, 180°. **e**, Relative approach/retreat velocity after mock-SFC and SFC. Note faster approach than retreat to CS⁻ and faster retreat than approach to CS⁺ after SFC (Methods; two-way repeated measures ANOVA—cohort × arena half, $F(1,100) = 117.05$, $P = 1.6 \times 10^{-18}$). **f**, Frequency of approach-avoidance behaviors toward CS⁺ (open bars, solid lines) and CS⁻ (filled bars, dashed lines) after mock-SFC or SFC. Two-sided Kolmogorov–Smirnov test, $^{****}P = 8.1 \times 10^{-5}$. **g**, Timeline of chemogenetic experiment. **h**, Left, Cre⁻ but not Cre⁺ (dCA2-silenced) cohort interacted more with CS⁻ than CS⁺ (two-way repeated measures ANOVA—cohort × stimulus mouse, $F(1,76) = 32.92$, $P = 1.85 \times 10^{-7}$). CS⁺ interaction times are similar between groups ($P = 0.071$; Bonferroni post hoc test). Right, discrimination scores. **h**–**l**, $n = 10$ *Avpr1b-Cre*⁻, $n = 10$ *Amigo2-Cre*⁻, $n = 10$ *Avpr1b-Cre*⁺ and $n = 10$ *Amigo2-Cre*⁺. **i**, Cartoon illustrating CS⁺ selective approach-avoidance behaviors for Cre⁻ but not Cre⁺ group. **j**, Velocity versus head orientation angle plots show Cre⁻ mice (purple) but not Cre⁺ mice (orange) selectively retreated from CS⁺ after SFC. **k**, Relative approach/retreat velocity scores. Two-way repeated measures ANOVA—cohort × arena half, $F(1,76) = 200$, $P = 5.5 \times 10^{-23}$. **l**, Frequency of approach-avoidance events toward CS⁺ was greater than toward CS⁻ for Cre⁻ but not Cre⁺ group after SFC. Two-sided Kolmogorov–Smirnov test, $^{****}P = 2.4 \times 10^{-5}$. Box plots—central line, median; bottom and top edges, 25th and 75th percentiles; whiskers, most extreme data points (excluding outliers); dots, individual animals. Bonferroni post hoc and *t*-tests, as appropriate—$^{*}P < 0.05$, $^{**}P < 0.01$, $^{***}P < 0.001$ and $^{****}P < 0.0001$. Sex was approximately balanced across conditions, and no sex differences were observed (for statistical comparison between females and males, see Supplementary Table 1 and Extended Data Fig. 5a–f).

approach-avoidance event frequency during the SFC social recall trial (Fig. 2g–l). In these experiments, both Cre⁺ and Cre⁻ littermate controls were injected with Cre-dependent AAV to express hM4Di selectively in the Cre⁺ mice. Both groups were then injected with CNO 30 min before SFC. In agreement with the results of Fig. 1, the Cre⁺ (dCA2-silenced) group showed a marked inhibition in social fear discrimination memory relative to the Cre⁻ controls, evidenced by the similar times that dCA2-silenced mice spent in the CS⁺ and CS⁻ arena halves and interacting with the CS⁺ and CS⁻ mice (Fig. 2h). Of particular interest, the changes in behavior following dCA2 silencing reflected an increased fear response directed towards the CS⁻, apparent by the decrease in CS⁻ interaction time and the increase in CS⁻ approach-avoidance event frequency, relative to the control group (Fig. 2i–l). The nonselective fear response to the CS⁻ and CS⁺ after dCA2 silencing was not due

https://doi.org/10.1038/s41593-024-01771-8

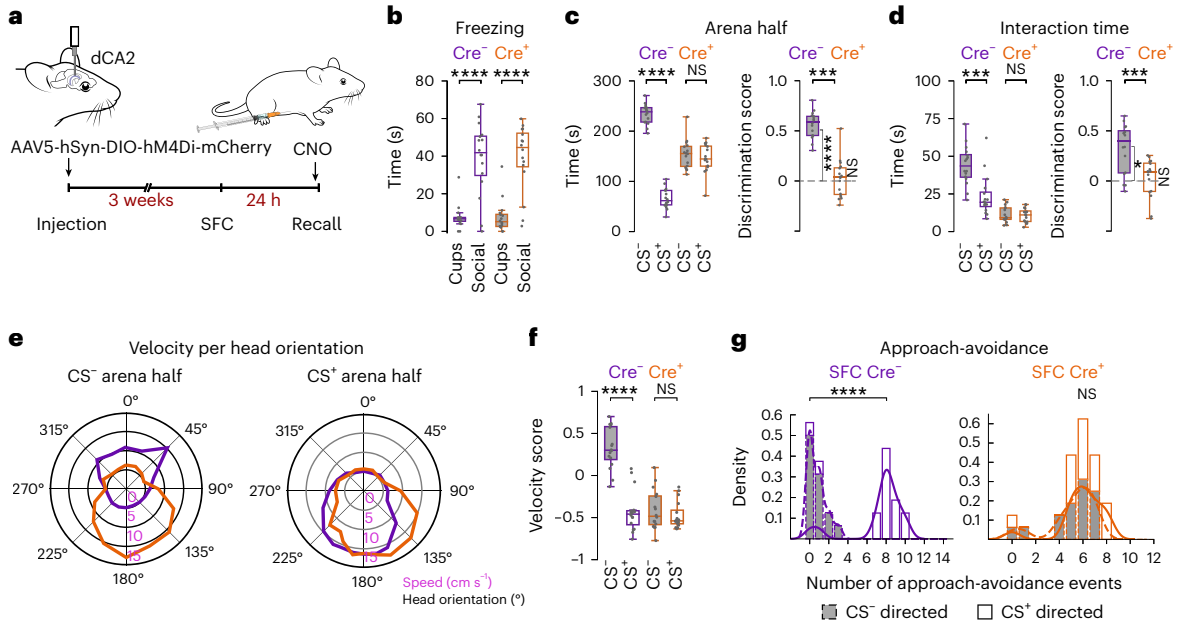

Fig. 3 | dCA2 pyramidal neuron activity is required for social fear discrimination memory during recall. a, Experimental timeline of chemogenetic silencing of dCA2 pyramidal neurons during SFC recall (day 2). **b**, Cre$^+$ mice and Cre$^-$ mice displayed comparable freezing durations (two-way repeated measures ANOVA—cohort × stage, $F(1,60) = 0.0001$, $P = 0.99$) that were significantly greater during social than cup recall trials. **b**–**g**, $n = 8$ *Amigo2-Cre*$^-$ and $n = 8$ *Avpr1b-Cre*$^-$; $n = 8$ *Amigo2-Cre*$^+$ and $n = 8$ *Avpr1b-Cre*$^+$. **c**, Left, Cre$^-$ but not Cre$^+$ mice selectively avoided the CS$^+$ arena half (left, two-way repeated measures ANOVA—cohort × arena half, $F(1,60) = 168.02$, $P = 4.48 \times 10^{-19}$). Right, discrimination scores. Discrimination scores for **c** and **d**—unpaired, two-sided *t*-tests between cohorts, two-sided one-sample *t*-tests against zero. **d**, Left, Cre$^-$ mice preferentially interacted with CS$^-$ relative to CS$^+$; Cre$^+$ mice showed little interaction with either (two-way repeated measures ANOVA—cohort × stimulus mouse, $F(1,60) = 15.46$, $P = 2.221 \times 10^{-4}$). CS$^+$ interaction times did not significantly differ between the Cre$^-$ and Cre$^+$ cohorts ($P = 0.068$, Bonferroni post hoc test). Right, discrimination scores. **e**, Velocity versus head orientation angle plots showing Cre$^-$ (purple) but not Cre$^+$ (orange) mice selectively retreat from CS$^+$. **f**, Relative approach/retreat velocity score (two-way repeated measures ANOVA—cohort × arena half, $F(1,60) = 37.45$, $P = 7.726 \times 10^{-8}$). **g**, Density plots show Cre$^-$ but not Cre$^+$ cohort had significantly more approach-avoidance events to the CS$^+$ than CS$^-$. Two-sided Kolmogorov–Smirnov test, $^{****}P = 3.1 \times 10^{-5}$. Box plots—central line, median; bottom and top edges, 25th and 75th percentiles; whiskers, most extreme data points (excluding outliers); dots, individual animals. Bonferroni post hoc and *t*-tests, as appropriate—$^*P < 0.05$, $^{***}P < 0.001$ and $^{****}P < 0.0001$. Sex was balanced across conditions, and no sex differences were observed (for statistical comparison between females and males, see Supplementary Table 1 and Extended Data Fig. 5a–f).

to generalized fear or anxiety, as the Cre$^+$ and Cre$^-$ groups showed similar low levels of freezing in the empty cup recall session and similar behaviors in the elevated plus maze or in locomotor activity (Extended Data Figs. 2b and 3c,d).

The difference in social fear discrimination between Cre$^+$ and Cre$^-$ mice was not due to their different genotypes, as separate control groups of Cre$^+$ and Cre$^-$ mice that did not express iDREADD and were injected with either saline or CNO before SFC showed similar behaviors (Extended Data Fig. 4). We saw a similar efficacy of dCA2 silencing in suppressing social fear discrimination memory in male and female subjects and when we used the *Amigo2-Cre* or *Avpr1b-Cre*[33] lines, demonstrating the generality of our findings (Extended Data Fig. 5). Finally, the effect of dCA2 silencing was not due to a decrease in the efficacy of the SFC protocol, as there was no significant difference in the number of foot shocks required for subjects to learn to avoid the CS$^+$ during the SFC learning trial when dCA2 was active or silenced (Extended Data Fig. 3e, f).

As CNO injection inhibits the activity of neurons expressing iDREADD for several hours during both SFC encoding and consolidation, we next used an optogenetic approach to selectively silence dCA2 during the SFC learning trial to examine its role specifically in SFC memory encoding. Similar to the chemogenetic results, we found that optogenetic silencing of dCA2 selectively during SFC encoding disrupted social fear discrimination memory during the recall session in Cre$^+$ relative to Cre$^-$ mice (Extended Data Fig. 6).

To investigate whether dCA2 activity was also required during the recall of social fear discrimination memory, Cre$^+$ and Cre$^-$ cohorts were injected with Cre-dependent iDREADD AAV in dCA2 and subjected to SFC in the absence of CNO. Both groups of mice were then injected with CNO 30 min before the 24 h recall sessions (Fig. 3). Similar to what we observed when we silenced dCA2 during SFC learning, silencing dCA2 during recall did not alter the increased freezing relative to the cup recall trial (Fig. 3b). However, dCA2 silencing during recall was sufficient to suppress social fear discrimination memory (Fig. 3c,d), with increased social avoidance of the CS$^-$ (Fig. 3e–g) relative to the Cre$^-$ control group.

As rodents adapt their behavior to potential threats through social observation[34], the ability of a subject to discriminate the CS$^+$ from CS$^-$ might, in principle, depend on acquired fear behaviors displayed by the CS$^+$. However, we found that when mock-SFC mice interacted with the same CS$^+$ and CS$^-$ used as stimulus mice in previous SFC trials with other subject mice, they failed to discriminate between the CS$^+$ and CS$^-$. Moreover, chemogenetic silencing of dCA2 to impair the social memory of the CS$^+$ and CS$^-$ mice during SFC did not alter the subject's preference (Extended Data Fig. 7). Thus, the ability of the subject to discriminate the CS$^+$ from the CS$^-$ most likely depends on the memory of the subject for the differing valences of the stimulus mice.

To assess whether dCA2 was specifically required for *social* aversive learning, we performed an analogous object fear conditioning (OFC) protocol, in which mice received a foot shock when interacting with one of two novel objects (Fig. 4). Similar to SFC, OFC mice, but not mock-OFC mice, displayed increased freezing when re-exposed to the objects after 24 h and spent significantly more time interacting with the CS$^-$ than the CS$^+$ object (Fig. 4c,d). Also similar to SFC, OFC mice displayed increased approach-avoidance behaviors toward the CS$^+$ relative to the CS$^-$ object (Fig. 4e–g). However, in stark contrast to SFC, chemogenetic silencing of dCA2 during the OFC learning trial did

https://doi.org/10.1038/s41593-024-01771-8

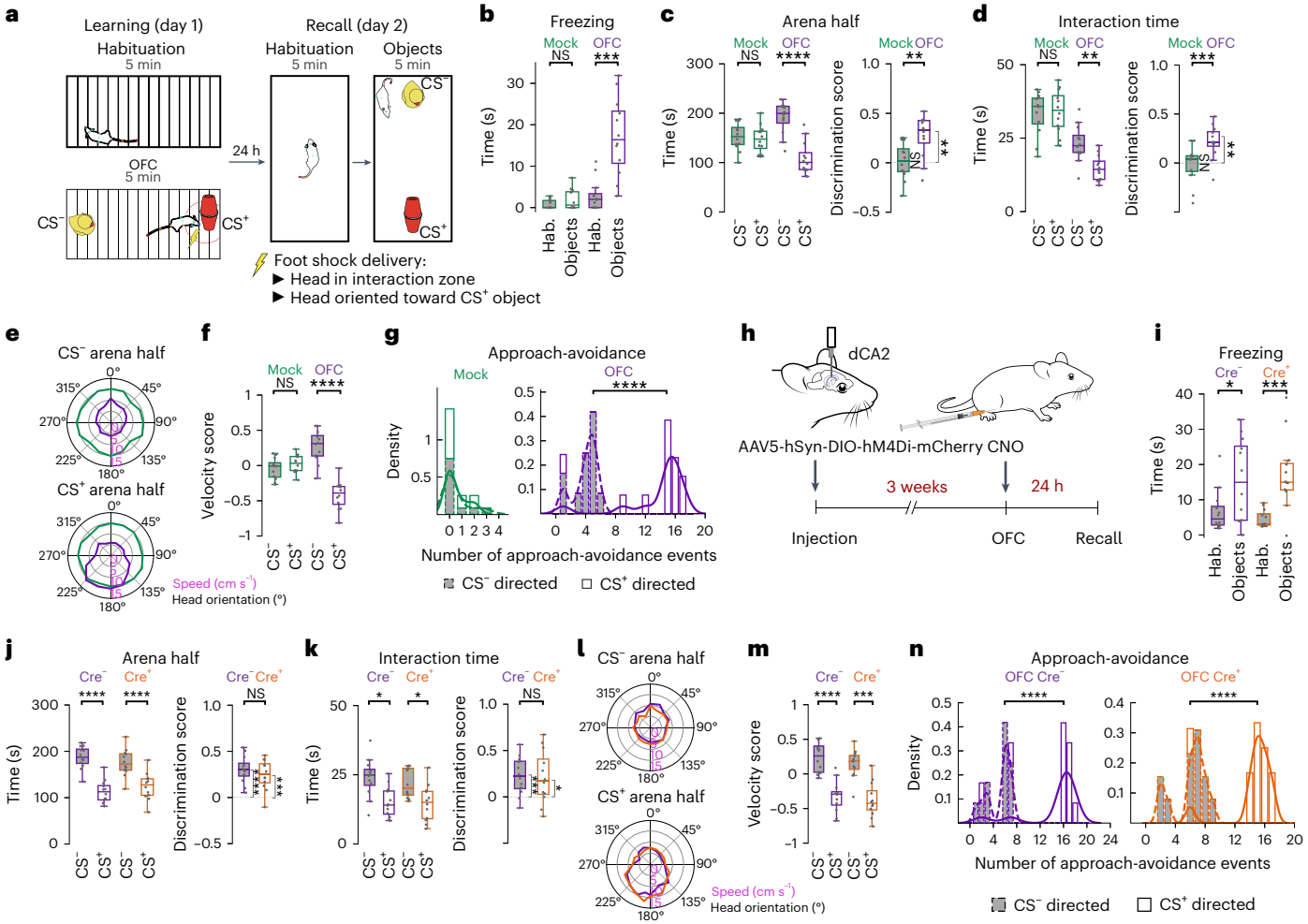

Fig. 4 | dCA2 pyramidal neurons are not required for object fear discrimination memory. a, OFC paradigm. **b**, OFC but not mock-OFC cohort displayed increased freezing during object recall relative to the habituation trial (two-way repeated measures ANOVA—cohort × stage, $F(1,44) = 18.797$, $P = 8.335 \times 10^{-5}$). **b**–**g**, $n = 12$ C57BL/6J wild-type mice per cohort. **c**, Left, OFC but not mock-OFC mice selectively avoided the CS$^+$ arena half (two-way repeated measures ANOVA—cohort × arena half, $F(1,44) = 19.36$, $P = 6.8 \times 10^{-5}$). Right, discrimination scores. Discrimination scores for **c**, **d**, **j** and **k**—unpaired, two-sided *t*-tests between cohorts; two-sided one-sample *t*-tests against zero. **d**, Left, OFC but not mock-OFC cohort interacted more with the CS$^-$ than CS$^+$ object (two-way repeated measures ANOVA—cohort × stimulus object, $F(1,44) = 6.1$, $P = 0.017$). Right, discrimination scores. **e**, Speed versus head orientation angle plot. **f**, Relative approach/retreat velocity score for mock-OFC and OFC groups (two-way repeated measures ANOVA—cohort × arena half, $F(1,44) = 51.87$, $P = 5.781 \times 10^{-9}$). **g**, Frequency of approach-avoidance events, two-sided Kolmogorov–Smirnov test, $^{****}P = 9 \times 10^{-5}$. **h**, Experimental timeline of chemogenetic experiment. **i**, Cre$^+$ (dCA2-silenced) and Cre$^-$ controls injected with CNO 30 min prior to OFC displayed comparably elevated freezing during object recall relative to the habituation trial (two-way repeated measures ANOVA—cohort × stage, $F(1,44) = 0.694$, $P = 0.409$). **i**–**n**, $n = 12$ *Amigo2-Cre*$^-$ and $n = 12$ *Amigo2-Cre*$^+$ mice. **j**, Left, Cre$^-$ and Cre$^+$ cohorts both avoided the CS$^+$ arena half (two-way repeated measures ANOVA—cohort × arena half, $F(1,44) = 2.096$, $P = 0.154$). Right, discrimination scores. **k**, Left, comparable CS$^-$ and CS$^+$ object interaction times between cohorts (two-way repeated measures ANOVA—cohort × stimulus object, $F(1,44) = 0.235$, $P = 0.629$). Right, discrimination scores. **l**, Cre$^-$ and Cre$^+$ mice exhibit similar selective retreat from CS$^+$. **m**, Relative approach/retreat velocity to CS$^-$ and CS$^+$ for Cre$^-$ and Cre$^+$ cohorts (two-way repeated measures ANOVA—cohort × arena half, $F(1,44) = 0.078$, $P = 0.78$). **n**, Frequency of approach-avoidance. Two-sided Kolmogorov–Smirnov test for CS$^-$ relative to CS$^+$, $^{****}P = 9.14 \times 10^{-5}$ and $^{****}P = 8 \times 10^{-5}$ for OFC Cre$^+$ and OFC Cre$^-$, respectively. Box plots—central line, median; bottom and top edges, 25th and 75th percentiles; whiskers, most extreme data points (excluding outliers); dots, individual animals. Bonferroni post hoc and *t*-tests, as appropriate—$^*P < 0.05$, $^{**}P < 0.01$, $^{***}P < 0.001$ and $^{****}P < 0.0001$. Sex was balanced across conditions, and no sex differences were observed (for statistical comparison between females and males, see Supplementary Table 1). Hab., habituation trial.

not impair object fear discrimination memory (Fig. 4h–n). Our finding that dCA2 was selectively important for the encoding and recall of social fear discrimination memory compared to object fear memory is consistent with previous results indicating a relatively selective role of dCA2 in socially relevant forms of memory[7,17].

dCA2 pyramidal cells encode the identity and valence of the CS$^+$ and CS$^-$ mice

We next investigated whether and how dCA2 represented social fear discrimination memory by imaging the calcium activity of dCA2 pyramidal neurons in subject mice as they explored stimulus mice before and after SFC. We expressed GCaMP8m in dCA2 pyramidal neurons using Cre-dependent AAV injections and recorded calcium dynamics in freely behaving mice through microendoscopic imaging (Fig. 5a–d). We first recorded dCA2 activity before SFC (day 1) as a subject mouse explored an open arena containing two empty cup cages. This was immediately followed by two social exploration (SE) imaging trials in which the subject explored two novel stimulus mice (in cup cages), whose locations were swapped between trials. After 2 h, the subjects underwent a mock-SFC trial in the SFC chamber. On day 2, we re-exposed the subjects to the open arena with empty cups, followed by four consecutive social recall (SR) imaging trials, with the positions of stimulus mice swapped

https://doi.org/10.1038/s41593-024-01771-8

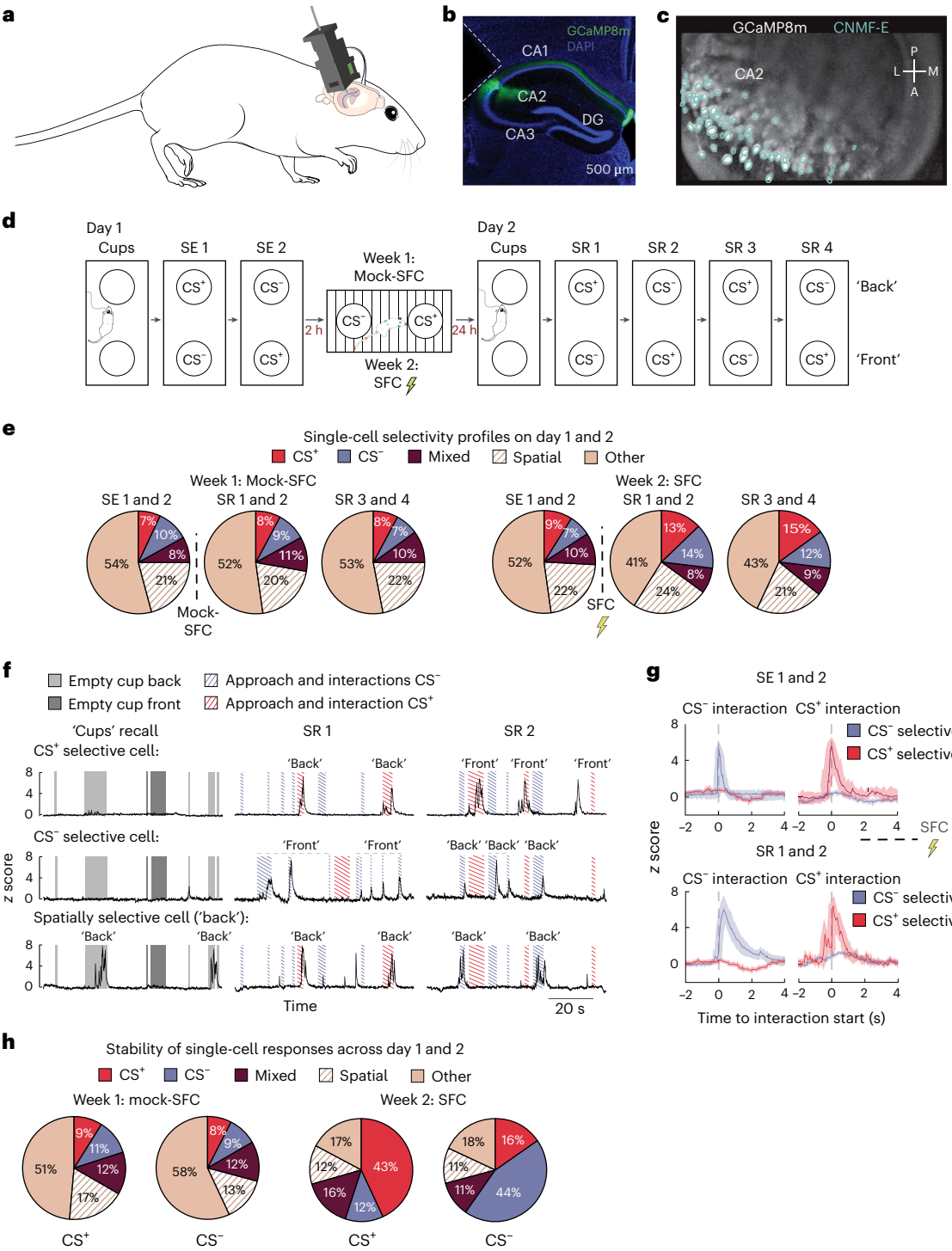

Fig. 5 | SFC enhanced and stabilized dCA2 pyramidal neuron representations of social identity. a, dCA2 pyramidal neuron microendoscopic calcium imaging. GCaMP8m is expressed in $n = 5$ male *Avpr1b-Cre*$^+$ and $n = 5$ male *Amigo2-Cre*$^+$ mice. **b**, Example GCaMP8m expression. Dashed lines, GRIN lens tract. **c**, Example field of view and cell detection with CNMF-E. **d**, Calcium imaging SFC paradigm. SE, social exploration trials 2 h before SFC or mock-SFC; SR, social recall trials 24 h after SFC or mock-SFC. **e**, Pie charts showing the fraction of dCA2 cells with indicated response selectivity during two SE trials before mock-SFC and SFC, and during four SR trials after mock-SFC or SFC. Fraction of CS$^+$ or CS$^-$ selective increased after SFC (two-sided chi-square test–$\chi^2(4) = 30.237$, $P = 4.38 \times 10^{-6}$) but not after mock-SFC (two-sided $\chi^2(4) = 3.364$, $P = 0.338$). **f**, Representative GCaMP8m *z*-scored activity traces as the subject mouse interacted with empty cups (left column) or a stimulus mouse during indicated SR trials after SFC (middle and right columns). Top row, CS$^+$ selective cell; middle, CS$^-$ selective cell; bottom, spatially selective cell. Shaded regions and labels indicate periods of interaction with an indicated cup ('back' or 'front' of the arena) or mouse. **g**, Average *z*-scored responses for CS$^-$ and CS$^+$ selective dCA2 cells during SE trials before and SR trials after SFC (mean ± s.e.m.; across mice) aligned to start of social interactions ($t = 0$; dashed line). **h**, CS$^+$ and CS$^-$ selective cells identified on day 1 (labels under the charts) showed an increased probability of maintaining their selectivity on day 2 after SFC (right) but not after mock-SFC (left). Two-sided chi-square tests, SFC for CS$^+$ cells–$\chi^2(4) = 24.307$, $P = 6.9 \times 10^{-5}$; for CS$^-$ cells–$\chi^2(4) = 21.409$, $P = 2.62 \times 10^{-4}$; mock-SFC for CS$^+$ cells–$\chi^2(4) = 0.8378$, $P = 0.933$; for CS$^-$ cells–$\chi^2(4) = 1.9028$, $P = 0.754$. Total number of cells (mean ± s.e.m. across mice)—mock-SFC SE, 672 (69 ± 14); mock-SFC SR, 658 (64 ± 10); SFC SE, 647 (62 ± 7) and SFC SR, 630 (58 ± 6). Stability analysis (**h**) based on tracking the same cell population across both days (mock-SFC, 658 cells; SFC, 630 cells total).

between each trial, which enabled us to disentangle dCA2 social and spatial information[17,32,35–37]. One week later, the same imaging protocol was repeated, but now with two novel stimulus mice 2 h before and 24 h after performing SFC, as described above.

We first compared the effects of SFC versus mock-SFC on the response profile of individual dCA2 pyramidal neurons, combining data from ten mice with an average of 65.2 ± 10 simultaneously imaged cells per mouse (mean ± s.d.; Fig. 5e,f). Before mock-SFC or SFC, a relatively small fraction of neurons showed a significant change in activity when the subject was interacting with a given stimulus mouse, relative to baseline activity levels during periods of nonsocial exploration ($P < 0.01$; Methods). Thus, 9.0% ± 3.2% (mean ± s.e.m.) of active dCA2 neurons responded selectively during periods of interaction with the prospective CS^+ mouse, and 7.0% ± 1.5% of cells responded selectively during exploration of the prospective CS^- mouse. An additional 8.0% ± 3.8% of cells showed mixed selectivity, responding during interactions with both CS^+ and CS^- mice.

Notably, SFC caused a significant increase in the fraction of CS^- and CS^+ selective cells. Thus, after SFC, the fraction of CS^+ selective cells increased to 13% ± 4.1%, and the fraction of CS^- selective cells increased to 14% ± 3.7% (chi-square test compared to before SFC, $\chi^2(4) = 30.237$, $P = 8.76 \times 10^{-6}$). In contrast, SFC caused no significant change in the fraction of mixed-selectivity cells ($\chi^2(4) = 3.364$, $P = 0.498$). In contrast to SFC, there was no change in the fraction of CS^+ or CS^- responsive cells or in the fraction of mixed-selectivity cells after mock-SFC (Fig. 5e). The fraction of CS^+ and CS^- selective cells also increased after SFC when we analyzed data in individual mice separately, although there was more variability (Extended Data Fig. 8). When we aligned the responses of the CS^+ and CS^- cells to the start of each social interaction bout, the event-triggered average activity for each group reached a peak near the start of the interaction (Fig. 5g, top row). After SFC, the CS^+ selective cells displayed an increase in calcium responses slightly before the start of an interaction, during the approach of the subject to the CS^+ (Fig. 5g, bottom row).

In addition to increasing the fraction of responsive cells, SFC caused a striking increase in the stability of response selectivity for both the CS^+ and CS^- responsive cells across the 2 days of the recordings compared to mock-SFC (Fig. 5h). Thus, only 8.5% of CS^+ cells and 7.5% of CS^- cells retained their selectivity for the same mouse before and 1 day after mock-SFC, similar to chance levels (8% and 9%, respectively; based on the fraction of CS^+ and CS^- selective cells on day 2). In contrast, 43% of CS^+ selective cells and 44% of CS^- selective cells retained their response selectivity after SFC, threefold greater than the chance levels of 13% and 14%, respectively (CS^+ cells—$\chi^2(4) = 24.307$, $P = 6.9 \times 10^{-5}$ and CS^- cells—$\chi^2(4) = 21.409$, $P = 2.62 \times 10^{-4}$).

dCA2 population activity encodes social threat and social safety

Although dCA2 population activity encodes both social novelty and social identity[17,36,37], it is not known whether social representations in dCA2 or any hippocampal region may be modified following an aversive social experience to encode social fear discrimination memory. We, therefore, used a linear support vector machine (SVM) classifier to assess whether dCA2 activity contained sufficient information to discriminate the CS^+ from the CS^- and whether this discrimination was altered after SFC. To construct binary classes for the CS^+ and CS^- that were independent of spatial location, we pooled calcium responses during equal times of interaction with a given stimulus mouse when it was in the front and back cups from two consecutive trials (Fig. 6a). To control for the interaction preference of the subject, we subsampled the data to include equal interaction times for the CS^+ and CS^-. We compared decoding accuracy to chance levels (~50%), determined for each animal as the average decoding accuracy performed on 1,000 random shufflings of the CS^+ and CS^- labels (Methods).

In line with previous work[37], conspecific identity could be decoded from dCA2 activity at levels significantly above chance, even before mock-SFC or SFC (Fig. 6a). Of note, SFC led to the avoidance of the CS^+ and preference for the CS^-, as described above, and significantly enhanced the accuracy of decoding the CS^+ from CS^- (Fig. 6a). Thus, decoding accuracy increased from 57.1% ± 1.15% in the SE trials before SFC to 67.7% ± 2.44% in the SR trials after SFC (mean ± s.e.m. for $n = 10$ mice; Bonferroni multiple comparisons test—SE 1 and 2 versus SR trials 1 and 2, $P < 0.01$; SE 1 and 2 versus SR 3 and 4, $P < 0.01$). In contrast, no significant change in decoding performance was observed after mock-SFC, where the mean decoding accuracy remained at ~60%. The increase in decoding accuracy was dependent on the 11% increase in the fraction of CS^+ and CS^- selective cells after SFC (Fig. 5e), as decoding accuracy after SFC was not significantly different from that before SFC when those cells were omitted from the post-SFC decoding analysis (Extended Data Fig. 9a,b). The decrease in accuracy was not simply a result of the decreased number of neurons used for decoding because we still observed a significant increase in decoding accuracy when we deleted a random set of 11% of cells after SFC. Our finding of enhanced decoding of conspecific identity following SFC is thus consistent with our single-cell analysis and suggests that past aversive social experiences are incorporated into dCA2 representations of conspecifics.

The increase in decoding accuracy following SFC is likely to be of behavioral relevance as it was strongly correlated with both the increase in freezing duration and the increase in CS^+/CS^- behavioral discrimination score during SR trials 1 and 2 (Fig. 6a,b). In contrast, there was not a significant correlation between increased decoding accuracy and either behavioral discrimination score or freezing in SR trials 3 and 4. We attribute the lack of correlation to the greatly diminished freezing and decreased avoidance of the CS^+ during trials 3 and 4, which may result from habituation or extinction of fear behavior due to the absence of a reinforcing stimulus during SR trials 1 and 2. That decoding accuracy remained high in the last two trials while fear behavior was greatly diminished indicates that the enhanced decoding of the CS^+ from CS^- following SFC is not simply a reflection of the differential fear response elicited by the stimulus mice. In contrast to the results with SFC, we observed no significant correlation between either type of behavioral readout and decoding accuracy for the mock-SFC cohort.

The enhancement in decoding of the CS^+ from CS^- could reflect a refinement in the representation of the CS^+ alone, the CS^- alone or both. To distinguish these possibilities, we used the SVM classifier to decode interactions with the empty cup (during the empty cup recall trial) compared to interactions with the cup in the same position in the social recall trials, when the cup contained either the CS^+ or CS^-. We found that the accuracy of decoding CS^+ and CS^- interactions versus their respective empty cup interactions were enhanced roughly equally after SFC, suggesting that the representations of both conspecifics were strengthened (Fig. 6c).

Next, we assessed whether SFC led to enhanced decoding of conspecific identity within a more naturalistic setting when the subject freely interacted with the CS^+ or CS^- in an open arena (Fig. 7a). Similar to when the stimulus mice were confined to cups, mice that underwent SFC, but not mock-SFC, freely interacted with the CS^- significantly more than the CS^+ (Fig. 7b,c). In addition, a linear SVM classifier successfully decoded periods when the subject approached or interacted with the CS^+ or CS^- compared to periods when the subject was not engaged in social interactions (matched for velocity and distance between subject and stimulus mice but with the head of the subject mouse oriented away from the stimulus mouse). Moreover, the accuracy of decoding increased significantly as the nose-to-nose distance between the subject and stimulus mouse decreased (Fig. 7d). Decoding accuracy of either stimulus mouse was significantly greater after SFC compared to mock-SFC. Moreover, after SFC the accuracy with which dCA2 activity decoded the presence of the CS^+ was significantly greater than that for the CS^-, especially at greater interaction distances. Thus, while dCA2

https://doi.org/10.1038/s41593-024-01771-8

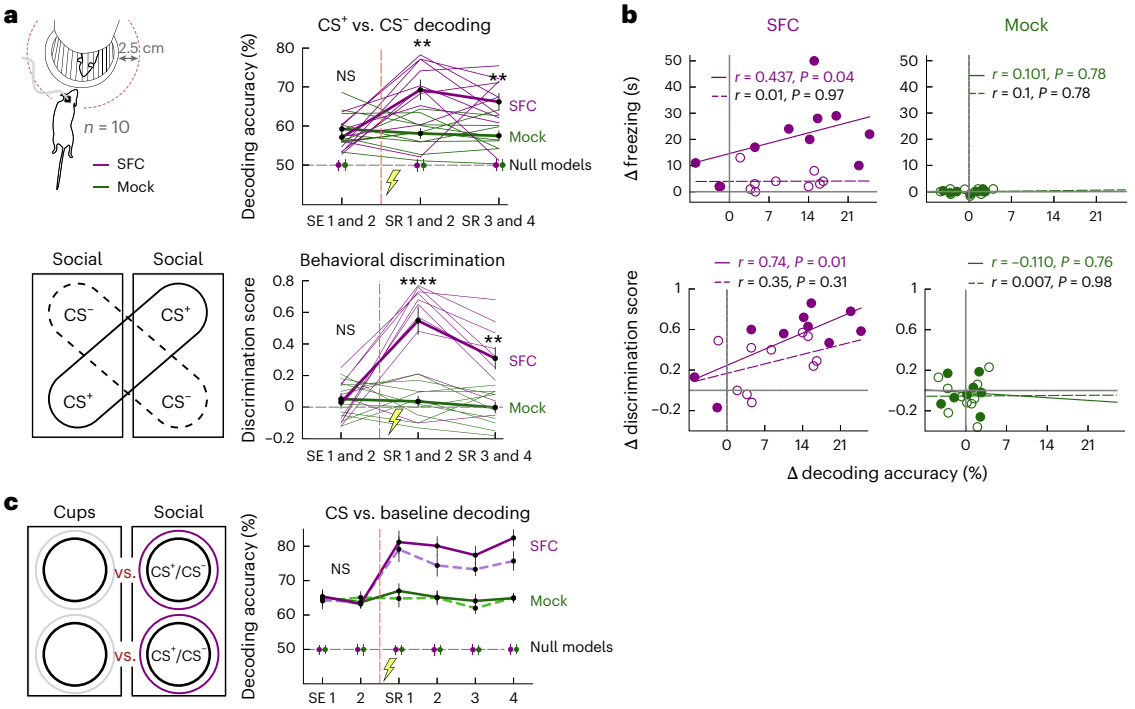

Fig. 6 | Enhanced decoding of CS$^+$ and CS$^-$ by dCA2 population activity after SFC. a, Top left, dCA2 pyramidal neuron activity based on calcium signals measured during interactions with stimulus mice. Bottom left, binary classes formed by grouping calcium signals for each neuron during exploration of CS$^+$ or CS$^-$ mice in front and back cups across two successive SE or SR trials. Top right, the accuracy of decoding interactions with CS$^+$ versus CS$^-$ during the two SE (SE 1 and 2) trials before mock-SFC (green) or SFC (purple), and during the two pairs of SR trials (SR 1 and 2, SR 3 and 4) after mock-SFC or SFC. Bottom right, behavioral discrimination scores for CS$^-$ versus CS$^+$ interaction times. Two-way repeated measures ANOVA—cohort × session. Decoding accuracy—$F(2,54) = 8.4$, $P = 6.67 \times 10^{-4}$ and discrimination score—$F(2,54) = 6.65 \times 10^{-4}$. Thin lines, individual animals. Filled symbols connected by thick lines and error bars in **a** and **c**, mean ± s.e.m. averaged from different animals for SFC, mock-SFC and null model as indicated. **a**–**c**, $n = 5$ male *Avpr1b-Cre*$^+$ and $n = 5$ male *Amigo2-Cre*$^+$ mice, 514 cells total. Bonferroni post hoc tests between SFC and mock-SFC, $^{**}P < 0.01$ and $^{****}P < 0.0001$ (see Supplementary Table 2 for P values of CS-decoding against the null model). **b**, Correlation between change in freezing time (top graphs) or behavioral discrimination score (bottom graphs) with change in decoding accuracy before and after SFC (left graphs) or mock-SFC (right graphs). Dots, individual animals. Filled symbols and solid lines, data from SR trials 1 and 2; open symbols and dashed lines, data from SR trials 3 and 4. r, Pearson's correlation coefficient. For SFC, both correlations were significant with SR trials 1 and 2 data; neither was significant for trials 3 and 4 data. For mock-SFC, no correlations were significant. **c**, Accuracy of decoding CS$^+$ (solid lines) or CS$^-$ (dashed lines) versus empty cup (same arena position) was enhanced after SFC but not mock-SFC (two-way repeated measures ANOVA—cohort × session, $F(5,108) = 4.717$, $P = 6.18 \times 10^{-4}$). Symbols and error bars show mean ± s.e.m. averaged from different animals. Significantly greater than chance decoding accuracies for SFC and mock-SFC for all trials. Significantly greater decoding accuracies after SFC versus mock-SFC on day 2 (one-sided, paired t-tests; see Supplementary Table 2 for P values across all trials).

activity successfully decoded the presence of the CS$^+$ when it was up to 5 cm away from the subject, the CS$^-$ could only be decoded at distances of 1.5 cm or less. In contrast, CA2 activity in the mock-SFC cohort could only decode the stimulus mice when they were within 0.5 cm, with no difference in decoding of either stimulus mouse.

As dCA2 encodes spatial as well as social information, we next asked whether SFC enhanced the accuracy of spatial decoding by pooling dCA2 activity data from interactions around the same cup location (that is, back or front cup) from two consecutive social exploration and social recall trials before and after SFC or mock-SFC. In line with previous work[37], we found that dCA2 activity allowed us to decode with above-chance-level accuracy spatial position (that is, front versus back cup location). However, unlike social decoding, spatial decoding accuracy did not significantly increase after SFC and was not correlated with behavioral discrimination of the CS$^+$ from CS$^-$ (Extended Data Fig. 9c–e).

As a further test of the behavioral relevance of the increase in stimulus mice decoding accuracy after SFC, we examined whether dCA2 representations of novel objects were modified following OFC, using a protocol similar to that used for SFC calcium imaging. The activity of a small fraction of dCA2 pyramidal neurons selectively responded as the subject interacted with one of the two stimulus objects before OFC. In addition, dCA2 representations were able to decode the two distinct objects at above-chance levels of accuracy. However, in contrast to SFC, dCA2 single-cell and population-level activity were not significantly modulated by object-valence associations, with no significant change in either the fraction of object selective cells or in object decoding accuracy (Extended Data Fig. 10). The differential effect of SFC and OFC on dCA2 pyramidal neuron representations mirrors the differential role of dCA2 in SFC and OFC behaviors, supporting the view that the changes in dCA2 activity we observed following SFC are likely to be of behavioral relevance.

dCA2 encodes an abstract representation of social valence

Our finding that SFC enhanced the ability of dCA2 representations to discriminate the CS$^+$ from CS$^-$ mouse prompted us to investigate whether SFC led to the incorporation of a representation of social valence into that of social identity. We used a linear classifier decoding approach to measure a quantity termed the cross-condition generalization performance (CCGP)[38], which required the use of training and testing datasets from distinct conditions, with two pairs of binary classes that differ in one common variable, in our case social valence. We therefore recorded calcium signals from the same set of dCA2 neurons as a subject mouse underwent two separate rounds of SFC,

https://doi.org/10.1038/s41593-024-01771-8

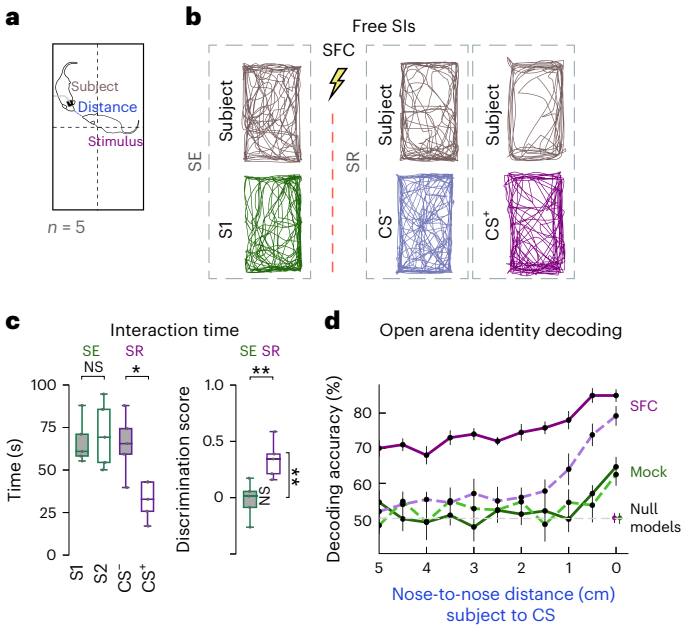

Fig. 7 | Enhanced decoding of stimulus mouse during free interactions after SFC. a, Subject and stimulus mice during free interactions in an open arena. **b**, Trajectories of the subject (top) and indicated stimulus mouse (bottom) during SE before SFC (left) and during two successive recall sessions with CS^- and CS^+ 24 h after SFC (right) with reduced social interactions during the latter. **c**, Left, subject mouse shows greater interaction time with CS^- relative to CS^+ after SFC; no difference before SFC (two-way repeated measures ANOVA—cohort × stimulus mouse, $F(1,60) = 15.46$, $P = 2.21 \times 10^{-4}$). Right, discrimination scores for CS^- versus CS^+ interaction times. Unpaired, two-sided *t*-tests between cohorts and two-sided one-sample *t*-tests against zero. **c**,**d**, $n = 5$ male *Amigo2-Cre*$^+$ mice, 382 cells total. **d**, CS^+ (solid lines) or CS− (dashed lines) decoding accuracy as a function of distance to subject mouse relative to no interaction at the same distance. After SFC (purple), CS^+ interactions decoded over a greater range of distances and with higher accuracy than CS^- interactions (dashed line; ANOVA—cohort × distance, $F(30,176) = 3.215$, $P = 6.13 \times 10^{-6}$). After SFC, CS^+ decoding accuracy was above the chance level at all distances. CS^- only was decoded above chance for separations ≤1.5 cm. CS^+ accuracy was significantly greater than CS^- accuracy at all distances. After mock-SFC (green), decoding accuracies for interactions with the two stimulus mice did not differ and were above chance only for separations ≤0.5 cm. Bonferroni post hoc tests and one-sided, paired *t*-tests against decoding accuracies obtained from the null model (see Supplementary Table 3 for *P* values across all distances). Bold lines and bars in **d**, mean ± s.e.m. across cohorts. Box plots—central line, median; bottom and top edges, 25th and 75th percentiles; whiskers, most extreme data points (excluding outliers); dots, individual animals. Bonferroni post hoc tests (**c**, left) and *t*-test (**c**, right), $^*P < 0.05$ and $^{**}P < 0.01$.

1 week apart, using different pairs of novel CS^+ and CS^- mice in each session (Fig. 8a). We measured CCGP from the accuracy with which a linear classifier trained to decode interactions with one pair of CS^+ and CS^- mice was able to decode the second pair of CS^+ and CS^- mice. As the identities of the four mice were distinct, the classifier trained on one pair of mice should only be able to decode the second pair of mice if dCA2 representations contained a generalized (that is, abstract) representation of social valence, the common variable.

With the two CS^+ and two CS^- mice from weeks 1 and 2 ($CS1^+$, $CS2^+$, $CS1^-$ and $CS2^-$) and the two recall trials per session (with positions of stimulus mice swapped), there were a total of eight conditions, providing a number of ways of assessing CCGP. We first determined CCGP using binary classes balanced for spatial location (back and front cups) and SFC session (weeks 1 and 2), as illustrated in Fig. 8b (grouping 1). Thus, we formed one training class by pooling dCA2 activity around $CS1^-$ in the recall trials of week 1 and the other training class by pooling dCA2 activity around $CS2^+$ in recall trials from week 2. We found that the classifier successfully decoded the similarly pooled test data from the pair of stimulus mice not used for training (CS^- from week 2 and CS^+ from week 1), yielding a high CCGP that was greater than chance at a high level of statistical significance (Fig. 8c). In contrast, CCGP was at chance levels when determined using a similar protocol with two pairs of mice that underwent mock-SFC.

In principle, a high CCGP could also be obtained if dCA2 representations encoded the passage of time between week 1 and week 2. However, in this case, grouping training and testing conditions by valence and not time would lead to a consistent assignment of the testing data to the wrong class used for training, resulting in CCGP levels significantly below chance (below 50% correct), inconsistent with the high CCGP we observed. That dCA2 did not encode the passage of time is further supported by the mock-SFC results, where CCGP determined across weeks 1 and 2 was not greater than chance.

Next, we investigated whether dCA2 population activity permitted the decoding of social valence irrespective of both social identity and spatial position of the CS^+ and CS^- mice (Fig. 8b (grouping 2)). We thus trained a classifier to decode one pair of CS^+ and CS^- mice in one cup location (for example, the back cup) and tested its performance on decoding a different pair of CS^+ and CS^- mice in the other cup location (for example, the front cup). The resultant CCGP was again significantly above chance after SFC, but not mock-SFC, despite the differences in spatial location and social identity in the training and testing groups (Fig. 8c). Similar to previous results[37], dCA2 also provided a generalized representation of spatial position independent of social identity or valence. Thus, a classifier trained to decode interactions with the back versus front cup containing a pair of stimulus mice of one valence could decode cup location when tested on data from a second pair of stimulus mice with the other valence (Fig. 8b (grouping 3) and 8c).

As SFC stabilized the single-cell responses to the CS^+ and CS^- from 1 day to the next, we next asked whether the coding of valence by single cells was maintained across the two pairs of mice over the 1-week interval between the two SFC sessions. We found that a significant fraction of cells that selectively responded during interactions with a mouse of a given valence after the first round of SFC maintained their selective valence responses when tested with the second pair of mice after the second round of SFC (Fig. 8d). Thus, both CCGP measures and single-cell analyses provide a consistent picture that dCA2 pyramidal neurons incorporate a generalized and stable encoding of valence into their representations of social identity following SFC.

The ability of a linear classifier to read out a generalized or abstract variable is a hallmark of low-dimensional representations in neural activity space[38] (Fig. 8e). In the simple scheme presented in Fig. 8e, we consider the representations of four individuals (two CS^+ and two CS^- mice) before and following SFC based on the mean firing rates of three hypothetical dCA2 neurons, with each individual represented as a distinct vector, or point, in three-dimensional neural activity space. In the least constrained geometrical arrangement, the four individuals are represented at four random locations in a tetrahedral three-dimensional geometry. Although a linear classifier can be trained to discriminate between any two individuals by constructing an appropriate decoding plane that separates the two clusters of points, there is no generalization as this decoding plane will not necessarily separate the other pairs of mice. Based on our CCGP results, we posit that the incorporation of social valence into dCA2 representations following SFC leads to a rearrangement in the geometry of neural activity so that the representations of animals with similar valence are now grouped closer to each other than are animals with different valences. This geometric arrangement after SFC predicts that the accuracy of decoding the identity of animals with the same valence should be less than that for animals with different valences, which is consistent with our pairwise decoding results presented in Supplementary Table 4.

https://doi.org/10.1038/s41593-024-01771-8

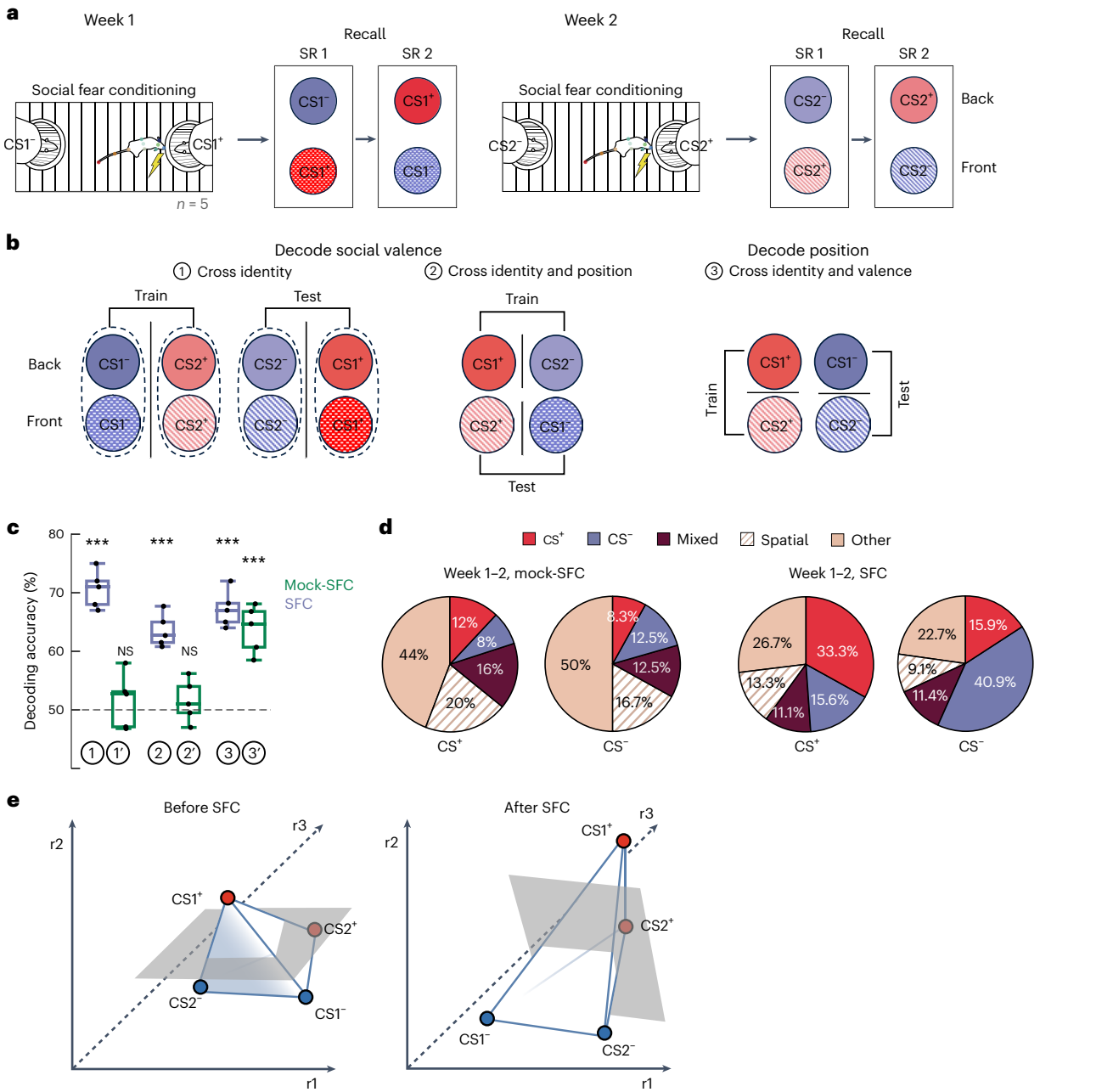

Fig. 8 | dCA2 population activity encodes an abstract representation of social valence and position. a, Protocol to measure CCGP. Two SFC sessions, separated by 1 week, with stimulus mice CS1$^+$ and CS1$^-$ in week 1 and CS2$^+$ and CS2$^-$ in week 2. CS$^-$ mice, blue; CS$^+$ mice, red. Week 1 mice, darker shades; week 2 mice, lighter shades. Back cup interactions, solid color; front cup interactions, cross-hatched. **b**, Assignment of binary classes for training and testing data to measure the following CCGPs: (1) cross-identity CCGP for social valence, (2) cross-identity and cross-position CCGP for social valence and (3) cross-identity CCGP for position. **c**, (1) Cross-identity social valence; CCGP = 70.6% ± 1.4% (mean ± s.e.m. throughout figure) after SFC (***$P = 3.11 \times 10^{-6}$ compared to null model, one-sided paired t-test throughout). CCGP = 51.5% ± 2.1% after mock-SFC (NS, $P = 0.97$). (2) Cross-identity and cross-position social valence; CCGP = 63.5% ± 1.3% after SFC (***$P = 1.2 \times 10^{-5}$). CCGP = 51.7% ± 1.8% after mock-SFC (NS, $P = 0.94$). (3) Position; CCGP = 67.2% ± 1.3% after SFC (***$P = 8.43 \times 10^{-6}$). CCGP = 63.8% ± 1.8% after mock-SFC (***$P = 2.17 \times 10^{-5}$). **c**,**d**, $n = 5$ male *Amigo2-Cre*$^+$ mice with 309 cells tracked across both SFC sessions. Box plots—central line, median; bottom and top edges, 25th and 75th percentiles; whiskers, most extreme data points (excluding outliers); dots, individual animals. **d**, Response profiles of dCA2 cells during week 2 mock-SFC or SFC recall sessions that were originally responsive to CS$^+$ or CS$^-$ (labeled below pie charts) during corresponding week 1 recall sessions. Two-sided chi-square tests against cell fractions expected by chance: mock-SFC CS$^+$—$\chi^2(4) = 5.2103$, $P = 0.266$; mock-SFC CS$^-$—$\chi^2(4) = 4.7123$, $P = 0.318$; SFC CS$^+$—$\chi^2(4) = 28.353$, $P = 1.1 \times 10^{-5}$ and SFC CS$^-$—$\chi^2(4) = 24.711$, $P = 5.8 \times 10^{-5}$. **e**, Hypothetical decoding plane from a linear classifier trained to decode CS1$^+$ from CS1$^-$ based on three-dimensional trapezoidal-like representational geometry before SFC (left) fails to separate (decode) CS2$^+$ from CS2$^-$. Classifier plane trained to decode CS1$^+$ from CS1$^-$ based on two-dimensional planar representations after SFC (right) will decode CS2$^+$ from CS2$^-$. Distances between points are drawn roughly to scale based on pairwise decoding results from Supplementary Table 4.

Discussion

Using a combined social-spatial fear conditioning paradigm, we find that independent neural processes underlie the ability of an animal to discriminate between spatial valence associations and social valence associations. Thus, while dCA1 pyramidal neurons are required for spatial but not social threat discrimination, consistent with their role in spatial reference memory and conditioned place aversion[39], dCA2 pyramidal neurons are required for social but not spatial threat discrimination. Although previous studies have implicated dCA2 in social novelty recognition memory[7–10] and the association of social odor with a water reward[40], our study demonstrates that dCA2 is also necessary for complex forms of episodic social memory requiring the association of specific individuals with a threatening or safe social experience. Our results also indicate that the two major components of social memory, the recognition of whether an individual is familiar or novel and the recollection and discrimination of previous experiences with equally familiar individuals[4,5,15,16], are mediated by a single class of neurons located in a relatively small brain subregion. Whether the same individual dCA2 neurons encode familiarity, socially associated reward and socially associated threat remains to be determined.

Another key finding of our study is the dissociation of the role of dCA2 in social fear discrimination memory from its lack of importance in associating threat with a general social context. Thus, subject mice exhibited a fear response to both threat- and safety-associated individuals when we silenced dCA2; however, the subject mice were not fearful during exposure to the empty cup cages that housed the stimulus mice during social recall trials. This suggests that brain regions outside of dCA2, such as those implicated in social fear responses following social defeat or a standard SFC protocol (that is, ventral hippocampus, amygdala, hypothalamus and lateral septum[22,41]), mediate the general association of social context with an aversive experience, with dCA2 required specifically to discriminate threat- from safety-associated individuals. The nonselective social fear phenotype of dCA2-silenced mice is reminiscent of social anxiety disorder, where fear responses are generalized to both safety- and threat-associated social contexts.

Our results also support the view that dCA2 has a relatively selective role in social forms of associative memory. Thus, while dCA2 was required for social fear discrimination memory after SFC, dCA2 was not necessary for object fear discrimination memory after OFC. Similarly, a previous study found that dCA2 was not required for nonsocial contextual fear conditioning in male mice[7], although it does have a role in female mice[42]. Moreover, we found that SFC, but not OFC, strengthened the ability of dCA2 representations to discriminate a CS^+ from CS^- (Figs. 6 and 7 and Extended Data Fig. 7). Our results that dCA2 is of particular importance for socially-related forms of memory are consistent with previous findings that dCA2 is required for social novelty recognition memory[7–10] but not for novel object memory[7,17] and that dCA2 is required for social odor-reward memory but not for nonsocial odor-reward memory[40]. Similarly, our results on dCA2 representations are consistent with findings that social odor-reward learning but not nonsocial odor-reward learning strengthens the ability of dCA2 representations to discriminate rewarded from unrewarded odors[40].

What neural circuits might enable the information within dCA2 to influence the behavioral discrimination of social threats from social safety? Results from previous studies suggest that both vCA1 and lateral septum are potential downstream targets. Thus, output from dCA2 to vCA1 contributes to social novelty recognition memory[10,14], whereas dCA2 outputs to lateral septum promote social aggression[43]. The latter action is of particular interest as it depends on the disinhibition of the ventrolateral subdivision of VMHvl[43], an area whose posterior subregion promotes social aggression while its anterior region regulates social avoidance[22,28,29]. vCA1 is also noteworthy as it contributes to both social novelty recognition memory[11,12] and regulates emotional behaviors through projections to diverse brain regions, including amygdala[41], nucleus accumbens[10], medial prefrontal cortex[12] and hypothalamus[44]. Further evidence implicating vCA1 comes from the finding that optogenetic activation of vCA1 social engram cells when paired with a foot shock can elicit a subsequent social fear response[11].

In principle, dCA2 could provide information solely about social identity to downstream brain regions, which would then associate a given social identity with threat or safety. Alternatively, dCA2 itself could participate in the association of valence with a specific individual's identity. We favor the latter possibility as SFC led to the incorporation of a generalized (that is, abstract) representation of social threat and social safety into dCA2 representations of social identity, based on a high CCGP, which is consistent with low-dimensional representations[37,38] of social valence (Fig. 8e). Of further note, our finding that a linear classifier yields a generalized decoding of social valence suggests a simple neurobiological implementation. Thus, a downstream neuron that linearly sums its dCA2 inputs with synaptic weights given by the decoding weights of the linear classifier can provide a generalized readout of social valence based on whether the inputs reach the threshold for driving neural output. Such a neuron could thereby provide social valence information to hard-wired circuits to trigger social approach or social avoidance behaviors independent of the specific social identity of a conspecific.

At present, it is unclear whether the same or distinct subpopulations of dCA2 neurons participate in social novelty recognition memory and social fear discrimination memory. For example, different subpopulations of dCA2 pyramidal neurons could mediate different social memory behaviors through projections to distinct dCA2 targets, including vCA1 and lateral septum, the latter important for regulating social avoidance[25,26]. Alternatively, a single population of dCA2 pyramidal neurons could mediate both forms of memory through the routing of dCA2 signals to distinct neural circuits based on the action of neuromodulators. This is consistent with findings that oxytocin and vasopressin contribute to social novelty recognition memory and social aggression through their actions in dCA2 (refs. 14,45–47) and lateral septum[43], respectively, and that oxytocin actions in lateral septum[25] and VMHvl[28] regulate social fear behaviors. Finally, the appropriate readout of the two forms of social memory could be achieved through distinct geometric representations in the activity space of a single population of dCA2 neurons that enable downstream neurons with appropriate synaptic weights to be differentially recruited by the distinct memory codes to elicit an appropriate social behavior.

Dysfunction in associative learning processes, such as the generalization of conditioned fear to neutral social stimuli, has been implicated in maladaptive social fear[1,2,26] and shown to underlie generalized social fear behaviors induced both by certain SFC and social defeat protocols[20,22,48]. Our finding that dCA2 silencing leads to a loss of the selective display of safety and fear behaviors toward appropriate social stimuli, together with findings of alterations in dCA2 properties in neuropsychiatric disorders in humans[49,50] and in mouse models of human disease[36,51], suggests a potential neural substrate for the social withdrawal and social fear generalization associated with such disorders. Future research on dCA2 may thus enhance our understanding of both the neural circuits mediating distinct memory processes and the etiology of social anxiety and other disorders related to the aberrant assignment of valence to social stimuli, with the promise of identifying new therapeutic approaches.

Online content

Any methods, additional references, Nature Portfolio reporting summaries, source data, extended data, supplementary information, acknowledgements, peer review information; details of author contributions and competing interests; and statements of data and code availability are available at https://doi.org/10.1038/s41593-024-01771-8.

References

1. Stein, M. B. & Stein, D. J. Social anxiety disorder. *Lancet* **371**, 1115–1125 (2008).
2. Beckers, T. et al. Understanding clinical fear and anxiety through the lens of human fear conditioning. *Nat. Rev. Psychol.* **2**, 233–245 (2023).
3. Ressler, K. J. et al. Post-traumatic stress disorder: clinical and translational neuroscience from cells to circuits. *Nat. Rev. Neurol.* **18**, 273–288 (2022).
4. Milner, B., Squire, L. R. & Kandel, E. R. Cognitive neuroscience and the study of memory. *Neuron* **20**, 445–468 (1998).
5. Wixted, J. T. & Squire, L. R. The role of the human hippocampus in familiarity-based and recollection-based recognition memory. *Behav. Brain Res.* **215**, 197–208 (2010).
6. Kogan, J. H., Frankland, P. W. & Silva, A. J. Long-term memory underlying hippocampus-dependent social recognition in mice. *Hippocampus* **10**, 47–56 (2000).
7. Hitti, F. L. & Siegelbaum, S. A. The hippocampal CA2 region is essential for social memory. *Nature* **508**, 88–92 (2014).
8. Stevenson, E. L. & Caldwell, H. K. Lesions to the CA2 region of the hippocampus impair social memory in mice. *Eur. J. Neurosci.* **40**, 3294–3301 (2014).
9. Smith, A. S., Williams Avram, S. K., Cymerblit-Sabba, A., Song, J. & Young, W. S. Targeted activation of the hippocampal dCA2 area strongly enhances social memory. *Mol. Psychiatry* **21**, 1137–1144 (2016).
10. Meira, T. et al. A hippocampal circuit linking dorsal CA2 to ventral CA1 critical for social memory dynamics. *Nat. Commun.* **9**, 4163 (2018).
11. Okuyama, T., Kitamura, T., Roy, D. S., Itohara, S. & Tonegawa, S. Ventral CA1 neurons store social memory. *Science* **353**, 1536–1541 (2016).
12. Phillips, M. L., Robinson, H. A. & Pozzo-Miller, L. Ventral hippocampal projections to the medial prefrontal cortex regulate social memory. *eLife* **8**, e44182 (2019).
13. Chiang, M. C., Huang, A. J., Wintzer, M. E., Ohshima, T. & McHugh, T. J. A role for CA3 in social recognition memory. *Behav. Brain Res.* **354**, 22–30 (2018).
14. Raam, T., McAvoy, K. M., Besnard, A., Veenema, A. H. & Sahay, A. Hippocampal oxytocin receptors are necessary for discrimination of social stimuli. *Nat. Commun.* **8**, 2001 (2017).
15. Eichenbaum, H., Yonelinas, A. P. & Ranganath, C. The medial temporal lobe and recognition memory. *Annu. Rev. Neurosci.* **30**, 123–152 (2007).
16. Yonelinas, A. P., Aly, M., Wang, W. C. & Koen, J. D. Recollection and familiarity: examining controversial assumptions and new directions. *Hippocampus* **20**, 1178–1194 (2010).
17. Oliva, A., Fernández-Ruiz, A., Leroy, F. & Siegelbaum, S. A. Hippocampal CA2 sharp-wave ripples reactivate and promote social memory. *Nature* **587**, 264–269 (2020).
18. Omer, D. B., Maimon, S. R., Las, L. & Ulanovsky, N. Social place-cells in the bat hippocampus. *Science* **359**, 218–224 (2018).
19. Danjo, T., Toyoizumi, T. & Fujisawa, S. Spatial representations of self and other in the hippocampus. *Science* **359**, 213 (2018).
20. Toth, I., Neumann, I. D. & Slattery, D. A. Social fear conditioning: a novel and specific animal model to study social anxiety disorder. *Neuropsychopharmacology* **37**, 1433–1443 (2012).
21. Padilla-Coreano, N., Tye, K. M. & Zelikowsky, M. Dynamic influences on the neural encoding of social valence. *Nat. Rev. Neurosci.* **23**, 535–550 (2022).
22. Diaz, V. & Lin, D. Neural circuits for coping with social defeat. *Curr. Opin. Neurobiol.* **60**, 99–107 (2020).
23. Masis-Calvo, M. et al. Animal models of social stress: the dark side of social interactions. *Stress* **21**, 417–432 (2018).
24. Xu, H. et al. A disinhibitory microcircuit mediates conditioned social fear in the prefrontal cortex. *Neuron* **102**, 668–682 (2019).
25. Zoicas, I., Slattery, D. A. & Neumann, I. D. Brain oxytocin in social fear conditioning and its extinction: involvement of the lateral septum. *Neuropsychopharmacology* **39**, 3027–3035 (2014).
26. Li, L. et al. Social trauma engages lateral septum circuitry to occlude social reward. *Nature* **613**, 696–703 (2023).
27. Markham, C. M., Taylor, S. L. & Huhman, K. L. Role of amygdala and hippocampus in the neural circuit subserving conditioned defeat in Syrian hamsters. *Learn. Mem.* **17**, 109–116 (2010).
28. Osakada, T. et al. A dedicated hypothalamic oxytocin circuit controls aversive social learning. *Nature* **626**, 347–356 (2024).
29. Krzywkowski, P., Penna, B. & Gross, C. T. Dynamic encoding of social threat and spatial context in the hypothalamus. *eLife* **9**, e57148 (2020).
30. Hartley, T., Lever, C., Burgess, N. & O'Keefe, J. Space in the brain: how the hippocampal formation supports spatial cognition. *Philos.Trans. R. Soc. Lond. B Biol. Sci.* **369**, 20120510 (2014).
31. Buzsáki, G., McKenzie, S. & Davachi, L. Neurophysiology of remembering. *Annu. Rev. Psychol.* **73**, 187–215 (2022).
32. Dudek, S. M., Alexander, G. M. & Farris, S. Rediscovering area CA2: unique properties and functions. *Nat. Rev. Neurosci.* **17**, 89–102 (2016).
33. Williams Avram, S. K. et al. NMDA receptor in vasopressin 1b neurons is not required for short-term social memory, object memory or aggression. *Front. Behav. Neurosci.* **13**, 218 (2019).
34. Silverstein, S. E. et al. A distinct cortical code for socially learned threat. *Nature* **626**, 1066–1072 (2024).
35. Mankin, E. A., Diehl, G. W., Sparks, F. T., Leutgeb, S. & Leutgeb, J. K. Hippocampal dCA2 activity patterns change over time to a larger extent than between spatial contexts. *Neuron* **85**, 190–201 (2015).
36. Donegan, M. L. et al. Coding of social novelty in the hippocampal CA2 region and its disruption and rescue in a 22q11.2 microdeletion mouse model. *Nat. Neurosci.* **23**, 1365–1375 (2020).
37. Boyle, L., Posani, L., Irfan, S., Siegelbaum, S. A. & Fusi, S. Tuned geometries of hippocampal representations meet the computational demands of social memory. *Neuron* **112**, 1358–1371 (2024).
38. Bernardi, S. et al. The geometry of abstraction in the hippocampus and prefrontal cortex. *Cell* **183**, 954–967 (2020).
39. Trouche, S. et al. Recoding a cocaine-place memory engram to a neutral engram in the hippocampus. *Nat. Neurosci.* **19**, 564–567 (2016).
40. Hassan, S. I., Bigler, S. & Siegelbaum, S. A. Social odor discrimination and its enhancement by associative learning in the hippocampal CA2 region. *Neuron* **111**, 2232–2246 (2023).
41. LeDoux, J. E. Emotion circuits in the brain. *Annu. Rev. Neurosci.* **23**, 155–184 (2000).
42. Alexander, G. M. et al. Modulation of CA2 neuronal activity increases behavioral responses to fear conditioning in female mice. *Neurobiol. Learn. Mem.* **163**, 107044 (2019).
43. Leroy, F. et al. A circuit from hippocampal CA2 to lateral septum disinhibits social aggression. *Nature* **564**, 213–218 (2018).
44. Jimenez, J. C. et al. Anxiety cells in a hippocampal-hypothalamic circuit. *Neuron* **97**, 670–683 (2018).
45. Caldwell, H. K., Wersinger, S. R. & Young, W. S. III The role of the vasopressin 1b receptor in aggression and other social behaviours. *Prog. Brain Res.* **170**, 65–72 (2008).
46. Cymerblit-Sabba, A. et al. Simultaneous knockouts of the oxytocin and vasopressin 1b receptors in hippocampal CA2 impair social memory. Preprint at *bioRxiv* 10.1101/2023.01.30.526271 (2023).
47. Pagani, J. H. et al. Role of the vasopressin 1b receptor in rodent aggressive behavior and synaptic plasticity in hippocampal area CA2. *Mol. Psychiatry* **20**, 490–499 (2015).
48. Ayash, S., Schmitt, U. & Müller, M. B. Chronic social defeat-induced social avoidance as a proxy of stress resilience in mice involves conditioned learning. *J. Psychiatr. Res.* **120**, 64–71 (2020).

49. Benes, F. M., Kwok, E. W., Vincent, S. L. & Todtenkopf, M. S. A reduction of nonpyramidal cells in sector CA2 of schizophrenics and manic depressives. *Biol. Psychiatry* **44**, 88–97 (1998).
50. Knable, M. B., Barci, B. M., Webster, M. J., Meador-Woodruff, J. & Torrey, E. F. Molecular abnormalities of the hippocampus in severe psychiatric illness: postmortem findings from the Stanley Neuropathology Consortium. *Mol. Psychiatry* **9**, 609–620 (2004).
51. Piskorowski, R. A. et al. Age-dependent specific changes in area CA2 of the hippocampus and social memory deficit in a mouse model of the 22q11.2 deletion syndrome. *Neuron* **89**, 163–176 (2016).

Methods

Animals

All experiments were approved by the Institutional Animal Care and Use Committee at Columbia University under protocol number AABJ7554. Adult male and female mice (8–14 weeks old) were maintained on a 12-h light/12-h dark cycle with ad libitum access to food and water. Subject mice used for all experiments were either from the C57BL/6J strain (Jackson Laboratories, 000664) or transgenic mice on the C57Bl/6J background. *Amigo2-Cre*[7] or *Avpr1b-Cre*[33] (Jackson Laboratories, 036876) mice, and their wild-type littermates (all on a C57BL/6J background) were used for optogenetic and chemogenetic dCA2 silencing and dCA2 miniscope imaging experiments. No statistically significant differences between outcome variables were observed with respect to sex or between *Amigo2-Cre* and *Avpr1b-Cre* mice (Extended Data Fig. 5). Thus, data obtained from these cohorts were pooled. Stimulus mice were age-, sex- and weight-matched to subject mice and from the C57BL/6J or *Cre* strains in experiments where dCA2 was chemogenetically silenced in stimulus mice during social fear conditioning. Sample sizes were not predetermined, but our sample sizes are similar or larger to those in previous studies[17,20,36,37]. Experimenters were blind to animal genotypes, and mice were randomly assigned to a given group within the experimental conditions. The order of experimental trials was randomized. Stimulus mice and stimulus objects were randomly designated as the 'CS^{+}' or the 'CS^{-}' for individual experimental trials. The positions of the stimulus mice were chosen at random for recall and swapped for experiments where further recall sessions followed. Subjects with mistargeted viral injections and/or optic fibers were excluded from analyses. In addition, mice with fewer than 50 pyramidal neurons on day 1 of an experiment were excluded from the analyses, as well as mice that exhibited freezing for over 80% (240 s) of recall (<5% of total), which reduced interaction times and/or the number of calcium events during social interactions to levels that were too low to quantify.

Viral injections and surgical procedures

Mice were anesthetized with isoflurane and administered analgesics for all surgical procedures. Stereotaxic injections were performed using a nano-inject II (Drummond Scientific). The pipette was retracted 8 min after stereotaxic injection, and after stereotaxic surgeries, viruses were allowed to incubate for 3–4 weeks before behavioral testing.

Pharmacogenetic silencing of dCA1 and dCA2

For the chemogenetic silencing of dCA2 pyramidal neurons[10,42], Cre-dependent AAV2/5 hSyn.DIO.hM4D(Gi)-mCherry (Addgene, 44362-AAV5) expressing the inhibitory hM4Di designer receptor exclusively activated by designer drugs (iDREADD) was injected bilaterally in the dCA2 region of *Amigo2-Cre* or *Avpr1b-Cre* mice. A volume of 200 nl of virus (1.9×10^{12} pp ml^{-1}) was injected per hemisphere at anteroposterior (AP), −2.0 mm; mediolateral (ML), +/−1.8 mm and dorsoventral (DV), −1.5 mm from Bregma. For the chemogenetic silencing of dCA1 pyramidal neurons, Cre-dependent AAV2/8 hSyn.DIO.hM4D(Gi)-mCherry (Addgene, 44362-AAV8) was injected bilaterally in the dCA1 region of *Lypd1-Cre* mice. A volume of 300 nl of virus (1.9×10^{12} pp ml^{-1}) was injected per hemisphere at AP, −1.9 mm; ML, ±1.5 mm and DV, −1.0 mm from Bregma. Wild-type littermates injected with the same AAV hSyn.DIO.hM4D(Gi)-mCherry or Cre^{+} littermates injected with mCherry were used as controls. For the spatio-social fear conditioning paradigm (Fig. 1), mCherry controls were approximately evenly split between dCA1 and dCA2 injections in *Lypd1-Cre* versus *Amigo2-Cre* or *Avpr1b-Cre* mice, respectively. For CNO versus saline control experiments (Extended Data Fig. 4i–r), *Avpr1b-Cre* mice were injected bilaterally in the dCA2 region with 200 nl of AAV2/5 hSyn-mCherry (Addgene, 114472-AAV5) in each hemisphere and with dCA2 coordinates as noted above.

Optogenetic silencing of dCA2

For optogenetic silencing of dCA2 pyramidal neurons, AAV2/2-EF1a-DIO-eArch3.0-eYFP ($1.9 \times 1{,}012$ pp ml^{-1}) was injected bilaterally in the dCA2 region of *Amigo2-Cre* or *Avpr1b-Cre* mice and wild-type littermate controls. A volume of 200 nl of virus (1.9×10^{12} pp ml^{-1}) was injected per hemisphere at AP, −1.8 mm; ML, ±2.1 mm and DV, −1.4 mm from Bregma. One week after injections, optical fiber assemblies (200 µm core, 0.37 numerical aperture, 3 mm; RWD Life Science) were implanted and placed at AP, −1.8 mm; ML, ±2.1 mm and DV, −1.2 mm from Bregma. Fibers were permanently fixed using dental cement.

Miniscope surgeries

A volume of 200 nl of pGP-AAV2/5-syn-FLEX-jGCaMP8m-WPRE (1.9×10^{12} pp ml^{-1}; Addgene, 162378) expressing the genetically encoded calcium indicator GcaMP8m was injected into the dCA2 region of the right hemisphere at AP, −2.0 mm; ML, +1.8 mm and DV, −1.7 mm from Bregma of *Amigo2-Cre* or *Avpr1b-Cre* mice (7–8 weeks old). Two to three weeks after stereotaxic injection, a gradient refractive index lens (GRIN lens, Inscopix; 1.0 mm diameter, 4.0 mm height) was implanted. The skull was scored with a scalpel followed by a rectangular craniotomy (1.2 × 1.2 mm; centered at AP, −2.0 mm and ML, +2.2 mm). Following the craniotomy, the GRIN lens was lowered to a depth of DV −1.4 to −1.5 mm from Bregma at a 10° angle to position the lens surface parallel to the dCA2 pyramidal layer. Finally, the lens was secured in place using Metabond dental cement. One week after the lens surgery, a baseplate was placed over the lens and secured with Metabond dental cement to enable rigid attachment of the miniscope for in vivo behavioral recordings.

Immunohistochemistry

Mice were transcardially perfused using 0.9% saline, followed by 4% paraformaldehyde (PFA) diluted in phosphate-buffered saline (PBS). Brains were collected and incubated in 4% PFA overnight and washed thrice for 10 min in PBS the following day. Coronal sections (60 µm) were obtained with a Leica VT1000S vibratome and subsequently permeabilized and blocked for 2 h with 5% goat serum and 0.5% Triton-X in PBS at room temperature. Sections were incubated overnight with primary antibodies and diluted in 5% goat serum and 0.1% TritonX-100 in PBS, at 4 °C. The following day, sections were washed thrice for 10 min in PBS, followed by the application of secondary antibodies at room temperature for 4 h in 5% goat serum and 0.1% Triton-X in PBS. Neuronal somata were visualized with a stain against the Nissl substance by using the NeuroTrace 435/455 fluorescent dye (Invitrogen, N21479; 1:200). All secondary antibodies were raised in goats, purchased from Thermo Fisher Scientific, and diluted at 1:500. Sections were mounted using fluoromount (Sigma-Aldrich), and images were acquired at ×5 and ×20 resolution using an inverted confocal microscope (Zeiss, LSM 700) and processed using FIJI software.

For eYFP and mCherry labeling, the first incubation was performed with chicken anti-GFP (AVES Labs, GFP-1020; 1:1,000) and rabbit anti-RFP (Rockland, 600-401-379; 1:1,000). The secondary incubation was performed with anti-chicken conjugated to Alexa 488 (Thermo Fisher Scientific, A11039) and anti-rabbit conjugated to Alexa 568 (Thermo Fisher Scientific, A11011). For RGS14 and PCP4 labeling, the first incubation was performed with mouse IgG2a anti-RGS14 (UC Davis/National Institute of Health (NIH) NeuroMab Facility, 73-170; 1:50) and rabbit anti-PCP4 (Sigma-Aldrich, HPA005792; 1:400). The secondary incubation was performed with anti-mouse IgG2a or anti-rabbit conjugated to Alexa 488 (Thermo Fisher Scientific, A21131).

Analysis of viral expression

To confirm the selective expression of the AAVs in dCA2, the overlap between an expressed viral fluorescent marker and the dCA2-specific markers RGS14 or PCP4 was assessed.

Behavioral assays

Between all behavioral trials, the arena and wire cups were cleaned with 70% alcohol wipes, followed by cleaning with water and drying.

Behavioral assays conducted with male versus female mice were conducted with at least a 1-week break in between.

Social–spatial fear conditioning (SFC) and social fear conditioning (SFC) paradigm

Apparatus. A modular shuttle chamber (51 cm length, 25 cm width and 30 cm height; Coulbourn, Harvard Biosciences) was used for fear conditioning. The chamber was placed within an isolation cubicle for noise attenuation and connected to a precision shocker (Coulbourn H13-15 Precision Shocker). During recall, a rectangular arena (50 cm length, 25 cm width and 30 cm height; made in-house) was used. Imaging Source DMK 37BUX252 video cameras mounted for top–down recordings of fear conditioning or recall sessions were used for video recording at 30 Hz. Throughout all stages of the paradigm, 3D-printed cylinder-shaped plastic caps were placed on top of wire cage cups to prevent mice from climbing on top of the cups.

Subject mice. Mice were habituated to the animal facility for at least 1 week after arrival from the vendor. Habituation to handling (5 min d^{-1}), the conditioning room (2 h d^{-1}) and wire cage cups (2 h d^{-1}) took place for two consecutive days before the start of the behavioral tests. Mice were randomly assigned to the fear-conditioned experimental group or the unconditioned 'mock' control group, with the same behavioral paradigm being followed for the latter with the exception of foot shock delivery. Subject mice were singly housed beginning 2 h before the fear conditioning stage of the experiment to allow for habituation to the homecage and maintained singly housed throughout the behavioral paradigm to prevent social fear extinction due to exposure to social stimuli. Habituation, fear conditioning and recall sessions took place during the same time of the day during the light phase.

Stimulus mice. Stimulus mice went through the same habituation routine as subject mice but were additionally habituated to being placed underwire cage cups twice for 5 min on each habituation day. Stimulus mice were singly housed for 1 week before the social fear conditioning and throughout the paradigm to prevent odor cross-contamination with other mice. Two animals from distinct litters from the subject mice served as the social stimulus mice. The same two stimulus mice were typically used for a cohort of around ten subject mice and designated at random as either the CS^+ or the CS^- for each subject mouse. Stimulus mice and control mice were housed in distinct rooms within Columbia University's animal facility and kept separate throughout the entire experiment except for fear conditioning and recall phases. Stimulus mice were placed on plastic bases to prevent them from receiving foot shocks. Stimulus mice were new to the subjects during day 1 of all experiments carried out.

Social fear conditioning. Fear conditioning consisted of two phases of 5 min each. During a nonsocial 'cups' stage, mice were allowed to freely explore for 5 min the fear conditioning chamber containing two empty wire cage cups placed on opposite sides of the chamber. During the social fear conditioning stage, both wire cage cups were replaced by identical wire cage cups containing the stimulus mice. The two stimulus mice were randomly assigned as the CS^+ or the CS^- for each experimental mouse and placed at random on either the right or left side of the fear conditioning chamber. Subject mice that were conditioned received a foot shock (1-s duration, 0.7 mA pulsed direct current), which was manually delivered whenever a subject mouse was detected to interact with the CS^+ mouse, based on the criteria that the head of the subject mouse was both inside a social interaction zone, defined as an area within 2.5 cm of the cup containing the CS^+ mouse, and oriented toward the center of the CS^+ cup. The fear conditioning stage ended either after 5 min of explorations or when four-foot shocks had been administered, at which time the mice were returned to their homecage.

Spatial fear recall. Spatial fear recall trials were performed 24 h after fear conditioning in the same behavioral room and the same fear conditioning chamber. The spatial fear recall consisted of 5 min where subject mice were exposed to the fear conditioning chamber containing empty wire cage cups at opposite sides of the chamber.

Social fear recall. Social fear recall trials were performed 24 h after fear conditioning (Fig. 1 immediately after spatial fear recall) in the same behavioral room but in a novel arena, rotated by 90° with respect to the experimenter, with different lighting (red LED light strips) than the fear conditioning arena and with smooth acrylic flooring in place of the metal grid. Similar to the fear conditioning trial, a recall trial consisted of two phases of 5 min each. Subject mice were exposed to a nonsocial 'cups' recall stage, where mice were allowed to freely explore two empty wire cage cups placed on opposite sides of the arena. This was followed after approximately 2 min by a 5 min 'social' recall stage, where the subject mouse was exposed to the CS^+ and CS^- stimulus mice previously encountered during fear conditioning. CS^+ and CS^- positions (distal versus proximal parts of the arena, relative to the experimenter) were assigned at random for the first trial of the recall session. Their positions were then swapped for every consecutive trial with different subject mice.

Recall with free social interactions. We used an SFC paradigm where both the subject and one stimulus mouse (CS^- or CS^+) were freely moving during SE trials before SFC and during social recall trials 24 h after SFC (Fig. 7c,d). The order of separate exposures of the subject mouse to the CS^+ was randomized between animals.

SFC behavioral paradigm for miniscope recordings. Before calcium imaging sessions using a miniature head-mounted microscope (miniscope), mice were habituated with a dummy miniscope until comfortable. A commutator was used during all recording sessions to enable rotation of the miniscope cable, thus allowing mice to move freely in the arena. Before behavioral testing, mice were allowed to acclimate to the behavioral room for 2 h. A nVista 3.0 Inscopix miniaturized microscope was inserted into the baseplate and used to record fluorescence signals from dCA2 pyramidal neurons expressing GCaMP8m during free behaviors using Inscopix data acquisition software (30 frames per second, 50-ms exposure, 0.2–0.4 mW mm^{-2} illumination intensity). The focal plane was optimized for each mouse individually and maintained throughout all recording sessions. To align behavior and calcium videos, a 5-V TTL pulse was triggered from an AMi-2 Optogenetic interface at the start of calcium recordings through Anymaze software synchronous with behavioral video recordings, both acquired at a rate of 30 Hz. Habituation to room and handling was conducted as described for the SFC behavioral paradigm.

Miniscope recording experiments were performed in two behavioral paradigms, a mock-SFC paradigm and an SFC paradigm, separated by 1 week. In the mock-SFC paradigm, mice were allowed to explore for 5 min a recall arena containing two empty wire cage cups on opposite sides of the arena. Two novel stimulus mice were then placed under the cups, and the subject mouse was allowed to explore the arena for two additional 5-min trials, with the positions of the stimulus mice swapped between the two trials. Mice were then returned to their homecage for 2 h, after which they were allowed to explore the fear conditioning chamber with two empty cups for 5 min, followed by an additional exploration trial in which the same two stimulus mice were present in the cups, with positions randomly assigned to right or left cup. No shocks were delivered throughout the sessions. Mice were then returned to their homecage for 24 h and then re-introduced to the recall arena for a 5 min trial of exploration of the empty cups ('cups' stage). This was followed by four consecutive 5-min recall trials in which the same stimulus mice encountered the previous day were present in the cups ('social' stage). Trials were separated approximately by 2 min

when the arena was cleaned and the positions of the stimulus mice were swapped in each consecutive trial. After 1 week, mice underwent the SFC paradigm. The paradigm was similar to the mock-SFC paradigm except that subject mice were administered foot shocks during exploration of the designated CS^+ stimulus mouse in the fear conditioning chamber, as described above during social fear conditioning. The same behavioral analysis as for SFC mice was performed for the mock-SFC cohort for stimulus mice randomly designated as the 'CS^+' or the 'CS^-'. The positions of the stimulus mice were chosen at random for the first recall session and swapped for the following three recall sessions. The arena was quickly cleaned both before and between the recall session with the general cleaning procedure described above. All SFC recordings were performed with $n = 2$foot shocks administered.

Social memory assay. Subject mice were habituated for 20 min to a rectangular arena with two empty wire cups (radius 5 cm) on opposite sides for 4 days. After habituation on day four, two novel stimulus mice were placed under the wire cups. In learning trials, the subject mouse was allowed to explore the arena with the novel stimulus mice for 5 min followed by another 5 min of exploration with the positions of the stimulus mice swapped. The subject mouse was then placed into a holding cage, followed by re-introduction to the same arena 30 min later for a 5-min recall trial in which the arena again contained two cups, each with a stimulus mouse. One of the cups contained one of the now familiar stimulus mice encountered in the learning trials (*F*), chosen at random, and the other cup contained a third novel stimulus mouse (*N*). Social memory is manifest in the innate preference of the subject mouse to explore the more novel of the two stimulus mice. Social interaction was defined as times when the subject's head was oriented toward the center of a cup containing a stimulus mouse within a 7.5 cm radius of the cup center (1.5× the radius of the cup; social interaction (SI) zone). We measured the total social interaction time during the recall trial for mouse *n* and mouse *F* and used this to calculate the following social discrimination score as a measure of social memory:

$$\text{Discrimination score} = \frac{(\text{SI time around mouse } N) - (\text{SI time around mouse } F)}{(\text{SI time around mouse } N) + (\text{SI time around mouse } F)}$$

Elevated plus maze. Mice were transferred to the behavioral testing room 2 h before the experiment for habituation to the room. For testing, mice were placed in the center of an elevated plus maze (Harvard Apparatus; two enclosed arms with 15-cm high walls and two open arms, arms 65 cm long and 6 cm wide; maze elevated 40 cm from the floor) facing the open arm of the maze and away from the experimenter. Mice were allowed to explore the maze for 8 min. The position of the head was tracked with DeepLabCut to calculate the number of entries into each arm, the time spent in each arm and the distance traveled.

OFC paradigm. We performed an OFC experiment closely based on the SFC protocol, except we used two novel objects in place of the novel stimulus mice, and the objects were not placed under cups. Different objects made of plastic, rubber or wood (all about 10 cm tall and 5 cm × 5 cm wide) were used for the OFC paradigm and randomly assigned as the CS^+ or the CS^- for each experimental mouse. Both fear conditioning and recall stages were preceded by 5 min of exposure to the respective empty arena. OFC miniscope recordings were conducted in a similar manner to SFC miniscope recordings, as described above. The same behavioral analysis as for OFC mice was performed for the mock-OFC cohort for stimulus objects randomly designated as the 'CS^+' or the 'CS^-'.

Optogenetic dCA2 silencing during social fear conditioning or recall. Mice were habituated for 4 days to the optogenetic apparatus by being allowed to freely explore the fear conditioning or the recall arena for 20 min while being connected to fiber optic leads attached to an optic rotary joint (Doric Lenses) centered above the arena. For photostimulation of eArch3.0, ferrules were connected to a 532-nm laser diode (OEM Laser Systems). A Master-8 pulse stimulator (AMPI) was used to control the laser, which was adjusted to around 8 mW for somatic stimulation using a digital power meter console (Thorlabs). Green light was delivered continuously during the 5 min SFC encoding trial to inhibit dCA2 pyramidal neurons by activating eArch3.0 bilaterally expressed in dCA2 pyramidal neurons of *Amigo2-Cre* or *Avpr1b-Cre* mice. We used independent cohorts of mice to silence dCA2 during encoding or recall. Control wild-type littermates injected with the same Cre-dependent virus received identical light pulses.

Chemogenetic silencing of dCA1 or dCA2 during behavioral assays. To silence dCA2, 3–4 weeks after stereotaxic viral injections of AAV2/5 hSyn.DIO.hM4D(Gi)-mCherry, *Amigo2-Cre* or *Avpr1b-Cre* mice were habituated to scruffing and intraperitoneal (IP) saline injections for four consecutive days. To silence dCA1, 3–4 weeks after stereotaxic viral injections of AAV2/8 hSyn.DIO.hM4D(Gi)-mCherry, *Lypd1-Cre* mice were habituated to scruffing and IP saline injections for four consecutive days. Mice were then injected 30 min before behavioral experiments intraperitoneally with 5 mg kg^{-1} of the iDREADD agonist CNO (Cayman Chemical, 34233-69-7) and returned to their homecage until behavioral testing. The volumes of saline and CNO injections were matched between habituation and testing days.

Chemogenetic silencing of dCA2 in stimulus mice during behavioral assays. Social memory tests and SFC paradigms where dCA2 was silenced in *Avpr1b-Cre* stimulus mice were performed approximately 3–4 weeks after stereotaxic viral injections of AAV2/5 hSyn.DIO.hM4D(Gi)-mCherry in the dCA2 of the stimulus mice. Social memory tests were performed with intraperitoneal administration of CNO to the stimulus mice 30 min before the first social memory encoding session. One week later, a social memory test was conducted with the same stimulus mice and a new cohort of subject mice, whereas intraperitoneal saline injections were administered to the stimulus mice 30 min before the first social memory encoding session. For the SFC paradigm with dCA2-silenced stimulus mice (that is, the CS^+ and the CS^-), stimulus mice were administered intraperitoneal CNO 30 min before social fear conditioning (day 1 of the SFC paradigm). The same pair of CS^+ and CS^- mice received 1 week later intraperitoneal saline injection 30 min before social fear conditioning and was used for a new cohort of subject mice. Both the social memory and the SFC assays with dCA2-silenced stimulus mice were in addition conducted with a second pair of stimulus mice and independent cohorts of subject mice.

Behavioral analysis

Pose tracking with DeepLabCut. DeepLabCut software[52] (v.2.3) based on ResNet-50 was used for markerless pose estimation of social fear-conditioned and unconditioned control mice during the 'cups' and the 'social' stages of recall. DeepLabCut was trained based on the following markers on the body of the subject mouse: (1) tip of the nose, (2) left ear, (3) right ear, (4), center of head (between both ears), (5) left side of waist, (6) right side of waist, (7) body center, (8) base of the tail, (9) center of the tail and (10) tip of the tail and four additional markers indicating the corners of the arena, as well as two markers indicating the center of the wire cage cups placed on opposite sides of the arena. The training set was composed of 320 videos and a total of 2,000 labeled frames randomly sampled with the built-in *k*-means algorithm and run for 500,000 iterations. Coordinates predicted with a likelihood below 95% were replaced by interpolation. Manual labeling of markers was done with the experimenter blind to genotype and experimental conditions.

Head direction analysis. The head direction of mice was calculated based on the vector connecting the nose and body center. A subject

mouse was taken as being oriented toward a stimulus mouse when the center of the relevant wire cage cup was within 20° to either side of this vector. Social interactions were defined as times when the subject's head was oriented toward the center of a cup containing a stimulus mouse within a 7.5 cm radius from the cup center (1.5× radius of the cup radius).

Manual annotation of videos. Video labels for supervised classification were obtained through manual annotation with BORIS software[53], based on top–down video recordings obtained from the 'social' stage of recall trials from nonconditioned controls, social fear-conditioned mice and social fear-conditioned mice during chemogenetic silencing trials. Behaviors were categorized as (1) 'freezing' (no movement except for respiration and heartbeat for at least 1 s), (2) 'approach' (approach to a stimulus mouse in stretched posture with a velocity below 10 cm s^{-1}, ending with nose marker crossing the interaction zone), (3) 'avoidance' (rapid retreat from a stimulus mouse, that is, with a velocity of above 10 cm s^{-1} and crossing the midline of the arena), (4) 'tail rattling' (fast waving movement of the tail) and (5) 'other' for any other type of behavior. A total of 60 videos with a framerate of 30 Hz were annotated, resulting in a total number of 540,000 annotated frames. All annotations were carried out with the experimenter blind to the genotype and experimental condition.

Feature extraction for supervised and unsupervised classification of behaviors. The following behavioral features were used to classify the behaviors of the subject mice both in the presence and absence of social stimulus animals: (1) center of the head (calculated as the position between ear markers), (2) distance of body center to cup centers, (3) distance of head center to cup centers, (4) distance of nose to cup centers, (5–8) distance of the head to each of four corners, (9–12) distance of head to each of four walls, (13) distance between body center and nose, (14) distance between the base of tail and nose, (15) distance between the left and right waist, (16) speed of the subject mouse (running average over two frames), (17 and 18) head orientation angle of the subject mouse with respect to cup centers and (19) all x and y coordinates for the relevant markers as obtained with DeepLabCut.

Feature preprocessing. Behavioral features for supervised and unsupervised classification were normalized to the [0,1] range with Python's sklearn.preprocessing StandardScaler to account for variability in animal size and slight differences in camera position. Features with values outside the 1st and 99th percentiles were removed to exclude outliers.

Supervised classification of behaviors with a long short-term memory (LSTM) recurrent neural network. To classify behaviors into the five classes as described above, an LSTM recurrent neural network was implemented using Python's TensorFlow package to account for the sequential nature of behaviors. Manual annotations were used as the ground truth, and prediction relied on the behavioral features defined above. The LSTM model architecture comprised an input layer, the LSTM layer with 100 memory units and a fully connected softmax layer enabling multiclass classification. Custom Python code was implemented to generate sequences of 90 frames (3 s) with a shift of at least ten frames between consecutive sequences. Data were stratified such that train and test sets contained sequences extracted from different segments of the video set to minimize dependency. The Adam algorithm for gradient descent was used for optimization of the model together with the categorical cross-entropy loss function, and classification accuracy was used as the outcome metric. A dropout and recursive dropout of 0.2 were used for regularization. Shuffled datasets were generated by random permutations of the behavior labels. Python's scikit-learn kernel density estimation function was then used for visualizing the distribution of predicted behaviors.

Analysis of one-photon calcium imaging data

Preprocessing of one-photon calcium data. Videos of calcium-dependent fluorescence signals from separate sessions within 1 day were concatenated within Inscopix Data Processing Software as 'time series'. Time series were corrected for defective pixels and 4× spatially downsampled. Background fluorescence was removed using a spatial band-pass filter based on default parameter values, and fluorescence videos were motion-corrected to the mean image using the Inscopix motion correction algorithm. Cell identification was implemented with the Inscopix CaImAn implementation with the average cell diameter evaluated with the Inscopix measurement tool, with a minimum pixel correlation parameter of 0.9, a merging factor of 0.9 and a minimum peak-to-noise ratio of 15. Default values were used for all other parameters, and the temporal traces were normalized to dF/F, that is, the change of a cell's fluorescence normalized to the mean fluorescence across the entire recording.

Single-cell analysis of calcium data. Calcium signals were measured in 100 ms bins during periods when the subject mouse was in an interaction zone around a cup (either empty or containing a stimulus mouse) and oriented toward the center of a given cup. To determine whether the activity of a given neuron was modulated by social interactions, we compared the calcium signals when the subject mouse explored the CS^+ or CS^- to the calcium signals recorded during the same trial when the subject mouse was not engaged in social interactions. We used a nonparametric Wilcoxon rank-sum test to determine whether there was a significant difference in calcium signals during social exploration compared to nonsocial exploration periods. Cells whose activity during SE with the same stimulus mouse differed significantly from baseline activity ($P \leq 0.01$) during two consecutive social recall trials and across both spatial positions (back and front cup) were classified as CS^+ and/or CS^- selective, according to the nature of the responses. Cells that were both CS^+ and CS^- selective were classified as 'mixed selective'. Cells whose activity during SE was significantly different from baseline across one spatial position independent of stimulus mouse identity were classified as spatially selective.

Linear population decoding. We used SVM with a linear kernel to decode calcium responses using a Python implementation of the libsvm package[54] (libsvm3.23). We trained the decoder on a subset of 90% of the data and then tested the performance on a subset of 10% of data that was withheld from the training dataset (tenfold cross validation). Features were constructed by averaging the dF/F calcium fluorescence signals of each cell over 100 ms bins and by assigning labels to the samples according to the mouse's behavior (for example, social interaction with the CS^+ or the CS^-). Sample sizes were balanced by class and across mice. Training, validation and test sets were stratified to contain samples from distinct social interaction periods. To decode information on the social identity of the CS^+ versus the CS^+ independently of spatial location based on dCA2 calcium activity, binary classification was performed on data combined from two consecutive trials, where the positions of the CS^+ and the CS^- are swapped, with time spent exploring right and left cups balanced. To decode information on spatial position based on dCA2 calcium activity, binary classification was used with calcium data combined from social interactions around the back versus the front interaction zones of the arena, irrespective of the interaction partner (CS^+ or CS^-), with time spent exploring the two stimulus mice balanced. The binary SVM classifier was then used to decode spatial position (back versus front interaction zone). Decoding for free social interactions (Fig. 7) was implemented with the same scheme, except that binary classes were constructed based on instances where subject and stimulus mice were oriented toward each other versus when they were not, matched for distance and velocity of the moving agent. In addition,

social interaction times were matched between subject mouse positions in the four quadrants of the recall arena (Fig. 7a).

CCGP. To calculate the CCGP, a linear SVM was trained to dissociate a dichotomy under one set of conditions and tested on the same dichotomy on data from a different set of conditions. For example, to determine the CCGP for the dichotomy valence, we trained the classifier based on interactions with the $CS1^+$ versus $CS2^-$ and then tested that classifier for its ability to decode the interactions with the $CS2^+$ versus $CS1^-$ (Fig. 8b, '(1)') We then reversed training and test datasets and measured CCGP as the average decoding performance for the two determinations. For cross-identity and cross-position social valence CCGP (Fig. 8b '(2)') and cross-identity position CCGP (Fig. 8b '(3)'), training and test sets were constructed from data pairs with opposing nondecoding variables. For instance, when decoding cross-identity and cross-position social valence CCGP, one training set contained data from social interactions around the back cup, while one test set contained left-out data from social interactions with a different pair of CS^+ and CS^- around the front cup. The CCGP decoding was repeated with swapped training and test sets and for (2) and (3) with swapped nondecoding variable associations. The reported CCGP was calculated as the average decoding accuracy for all relevant training and testing schemes, whereby sample sizes were balanced across all possible classes. The CCGP null model was estimated by randomly shuffling neuron indices[37].

Permutation testing and empirical chance-level calculation. The empirical chance level was calculated for each animal by carrying out the tenfold cross-validated decoding as described above 1,000 times. However, classification labels were permuted for each of the $m = 1{,}000$ iterations, such that classification labels were randomly assigned to the feature vector (data samples averaged across 100 ms of calcium recordings)[55]. Thus, for each individual animal, 1,000 shuffled classification accuracies based on randomly permuted labels were obtained. On the group level, statistical significance was calculated by comparison of true classification accuracies ($n = 10$ values, one value per animal) versus chance-level accuracies averaged for each animal over the $m = 1{,}000$ permutations ($n = 10$ average chance-level accuracies, one value per animal) with a paired t-test. Visualized are chance-level accuracies and s.e.m. across $n = 10$ animals (Figs. 6 and 7).

Statistical analysis

All statistical analyses were implemented either in Python (v.3.11.1) or R (4.2.2). Data distribution was assumed to be normal, but this was not formally tested. One-way analysis of variance (ANOVA), two-way repeated measures ANOVA and t-tests were used where indicated. Midlines of box plots indicate median, while the range of the box plot indicates the back (75%) and lower (25%) quartiles. Box plot whiskers include data within a 1.5× interquartile range. A significance threshold of $\alpha = 0.05$ was used except when indicated differently, with not significant (NS) thus indicating $P > 0.05$ and the following used otherwise: $^*P < 0.05$, $^{**}P < 0.01$, $^{***}P < 0.001$ and $^{****}P < 0.0001$. All behavioral, imaging and optogenetics experiments were replicated in multiple subject animals with similar results.

Python packages

The majority of the code was implemented in Python and makes use of the following packages: 'os' (v2.1.4), 'sys' (v3.11.4) and 'utils' (v1.0.2) for system administration; 'numpy' (v2.0), 'scipy' (v1.14.0) and 'pandas' (v2.2.2) for data processing, data analysis and general data handling; 'scikit-learn' (v1.5.0) for preprocessing of the data for classification and k-means clustering; 'TensorFlow' (v2.11) and 'libsvm' (v3.23.0.4) for LSTM and SVM classification, respectively; 'Matplotlib' (v3.9), 'seaborn' (v0.11.2) and 'plotly' (v5.7) for data visualization. Plotly data visualization was used for polar plots based on modified custom code[56].

Reporting summary

Further information on research design is available in the Nature Portfolio Reporting Summary linked to this article.

Data availability

Datasets and analytical tools included in this study are available from the corresponding authors upon reasonable request. Source data are provided with this paper.

Code availability

Python code for underlying visualization and analysis can be obtained from https://github.com/Siegelbaumlab/dCA2_SFC.

References

52. Mathis, A. et al. DeepLabCut: markerless pose estimation of user-defined body parts with deep learning. *Nat. Neurosci.* **21**, 1281–1289 (2018).
53. Friard, O. & Gamba, M. BORIS: a free, versatile open-source event-logging software for video/audio coding and live observations. *Methods Ecol. Evol.* **7**, 1325–1330 (2016).
54. Chang, C.-C. & Lin, C.-J. LIBSVM: a library for support vector machines. *ACM Trans. Intell. Syst. Technol.* **2**, 1–27 (2011).
55. Davison, A. C. & Hinkley, D. V. *Bootstrap Methods and Their Application (No. 1)* (Cambridge University Press, 1997).
56. Ashaber, M. et al. Anatomy and activity patterns in a multifunctional motor neuron and its surrounding circuits. *eLife* **10**, e61881 (2021).
57. Tyler, E. & Kravitz, L. Mouse. *Zenodo* https://doi.org/10.5281/zenodo.3925901 (2020).
58. De Francesco, N. 1ml syringe with 25G needle. *Zenodo* https://doi.org/10.5281/zenodo.4912419 (2021).
59. Tyler, E. & Kravitz, L. Obese mouse walking. *Zenodo* https://doi.org/10.5281/zenodo.3926205 (2020).
60. Li, L. EPM. *Zenodo* https://doi.org/10.5281/zenodo.5496320 (2021).

Acknowledgements

We thank L. Abbott, S. Fusi, C. D. Salzmann, L. Posani, S. Hassan, R. Nguyen, R. Morais-Ribeiro and M. R. Whiteway for critical discussions and comments on the manuscript, C. de Solis for assistance with implementing preliminary SFC experiments and all members of the Siegelbaum Lab for assistance throughout the work. Mouse and needle schematics in Figs. 1b, 2g, 3a and 4a, and Elevated Plus Maze in EDF 3 are from SciDraw (https://doi.org/10.5281/zenodo.3925901 (ref. 57), https://doi.org/10.5281/zenodo.4912419 (ref. 58), https://doi.org/10.5281/zenodo.3926205 (ref. 59) and https://doi.org/10.5281/zenodo.5496320 (ref. 60)). The work from this publication was supported by the Swiss National Science Foundation (grants P2EZP3_181896 and P500PB_203063 to P.K.) and NIH (grants R01 MH104602 and R01 MH120292 to S.A.S.).

Author contributions

P.K. and S.A.S. conceived of the project and wrote the manuscript. P.K. designed and implemented the SFC paradigm, implemented software, analyzed the behavioral and neural data and performed all surgeries and behavioral experiments. S.K.B. performed the viral injections for the optogenetic experiments and optogenetic fiber implant surgeries. D.M.G.S. performed the immunohistochemistry, perfusions and confocal imaging for the optogenetic and OFC experiments and manually labeled behavioral videos for Figs. 2 and 3. N.S. performed the DeepLabCut analysis. A.B. performed immunohistochemistry experiments together with P.K. H.L. conceived of and generated the *Avpr1b-Cre* mouse line with guidance from W.S.Y.

Competing interests
The authors declare no competing interests.

Additional information
Extended data is available for this paper at https://doi.org/10.1038/s41593-024-01771-8.

Supplementary information The online version contains supplementary material available at https://doi.org/10.1038/s41593-024-01771-8.

Correspondence and requests for materials should be addressed to Pegah Kassraian.

Peer review information *Nature Neuroscience* thanks Clifford Kentros, Moriel Zelikowsky and the other, anonymous, reviewer(s) for their contribution to the peer review of this work.

https://doi.org/10.1038/s41593-024-01771-8

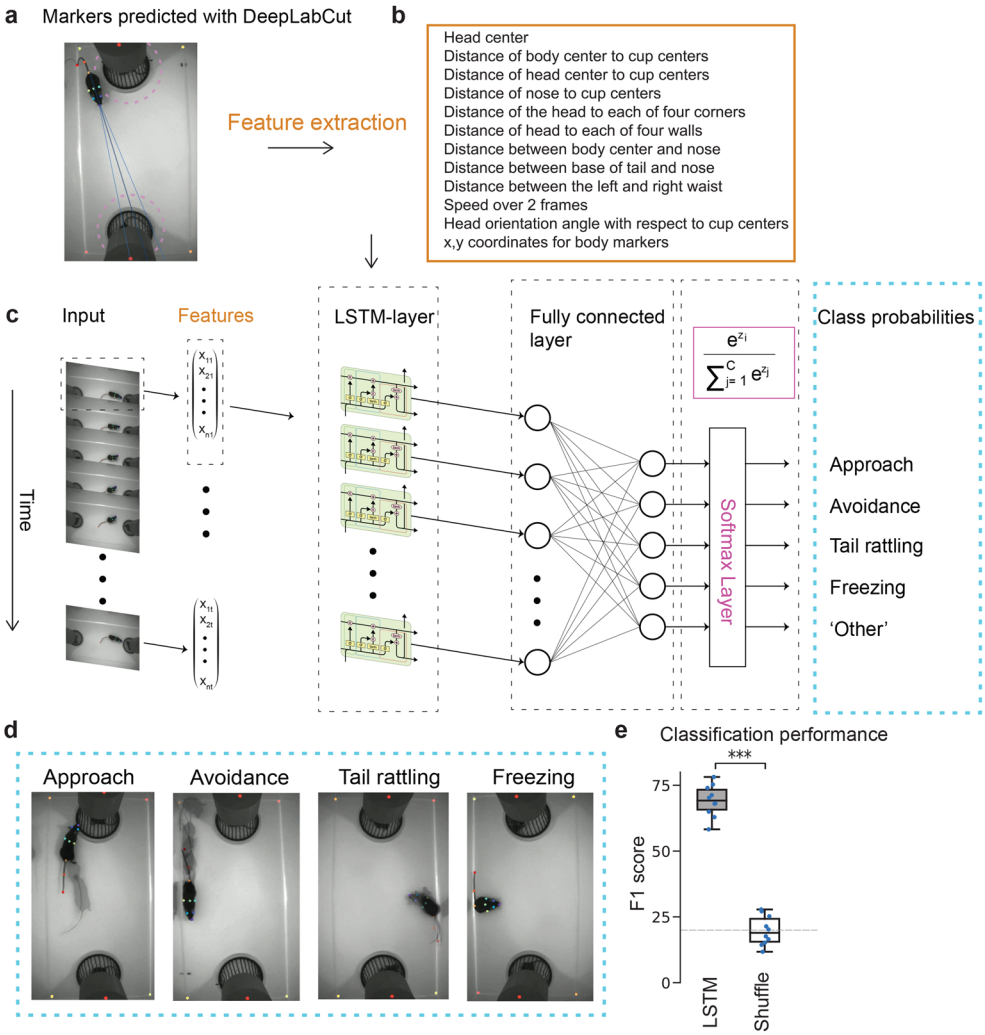

Extended Data Fig. 1 | Deep learning pipeline for the automated quantification of behavior. a, Markerless pose estimation during recall was implemented with DeepLabCut. Training of the ResNet-50 network was based on a total of 9 markers on the body of the subject mouse, 4 markers indicating the corners of the arena and 2 markers indicating the center of the wire cage cups placed on opposite sides of the arena as a proxy of stimulus mouse position. Dotted circles around cups illustrate the social interaction zone (1.5× the radius of the cup). Dark blue lines illustrate the head orientation of the subject mouse (see Methods for further details). **b**, Markers as predicted with DeepLabCut were employed to obtain features pertaining to posture of the mouse, its velocity and its position and orientation within the arena. **c**, To categorize behaviors into the five classes, a long short-term memory (LSTM) neural network was used to account for the sequential nature of behaviors, whereby manual annotations served as the ground truth. Illustration of the model for a single time frame, with the LSTM layer comprising 100 memory units (green) and input features described in **a**. The LSTM layer was followed by a fully connected softmax layer for the prediction of class probabilities. **d**, Example sequences illustrating behaviors of interest. Behaviors not falling into these categories were labeled as 'other'. **e**, F1 score calculated based on softmax output probabilities; shuffled control data based on randomly shifted frames were associated with significantly lower classification accuracies. F1 scores from 10-fold cross-validation. Two-sided Mann–Whitney $U = 100$, $^{***}P = 1.826 \times 10^{-4}$. Box plot: central line, median; bottom and top edges, 25th and 75th percentiles; whiskers, most extreme data points (excluding outliers); dots, decoding accuracies from 10-fold cross-validation.

https://doi.org/10.1038/s41593-024-01771-8

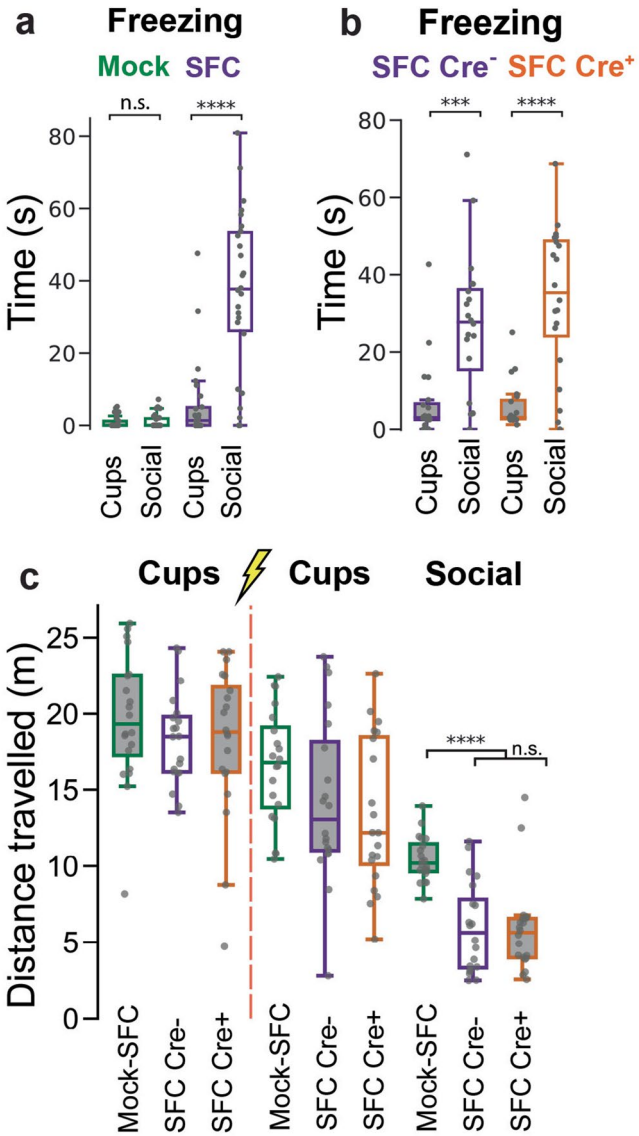

Extended Data Fig. 2 | See next page for caption.

https://doi.org/10.1038/s41593-024-01771-8

Extended Data Fig. 2 | SFC induces freezing and decreases distance traveled during social recall. a, Freezing duration for mock-SFC (green) and SFC cohorts (purple) during recall trials 24 h after SFC. SFC but not mock-SFC cohort displays elevated freezing duration during the 'social' recall trial relative to the non-social 'cups' recall trial 24 h after SFC (two-way repeated measures ANOVA: cohort × stage, $F(1,100) = 38.82$, $P = 1.104 \times 10^{-8}$). N = 26 C57BL/6J wild-type mice per cohort. **b**, Freezing duration for Cre^- (purple) and Cre^+ cohorts (orange; dCA2 silenced) during 'cups' and 'social' recall trials 24 h after SFC. Both cohorts display similar low freezing duration during 'cups' recall trials and similarly elevated freezing duration during 'social' recall trials (two-way repeated measures ANOVA: cohort × stage, $F(1,76) = 1.3846$, $P = 0.243$). N = 10 *Avpr1b-Cre*$^-$, N = 10 *Amigo2-Cre*$^-$, N = 10 *Avpr1b-Cre*$^+$, N = 10 *Amigo2-Cre*$^+$. **c**, Distance traveled (m) for mock-SFC (green), SFC Cre^- (purple) and SFC Cre^+ (orange) cohorts during 'cups' trial in the SFC chamber (before SFC; SFC marked by dashed vertical line) and during 'cups' and 'social' recall trials in novel recall arena 24 h after SFC. There was no significant difference in distance traveled among cohorts during 'cups' trial on day 1 before SFC. On day 2, mock-SFC cohort (green) showed significantly greater mobility during the 'social' recall trial than both Cre^- (purple) and Cre^+ (orange) SFC cohorts. Cre^- and Cre^+ cohorts did not differ significantly in terms of their mobility (two-way repeated measures ANOVA: cohort × stage, $F(4,171) = 1.35$, $P = 0.0113$). Data pooled and subsampled from Fig. 2; mock-SFC: N = 20 C57BL/6J wild-type mice; SFC Cre^-: N = 10 *Avpr1b-Cre*$^-$ and N = 10 *Amigo2-Cre*$^-$; SFC Cre^+: N = 10 *Avpr1b-Cre*$^+$ and N = 10 *Amigo2-Cre*$^+$. Bonferroni post hoc tests: *** $P < 0.001$, **** $P < 0.0001$, n.s.: not significant. Box plots: central line, median; bottom and top edges, 25th and 75th percentiles; whiskers, most extreme data points (excluding outliers); dots, individual animals. Sex is balanced per condition.

https://doi.org/10.1038/s41593-024-01771-8

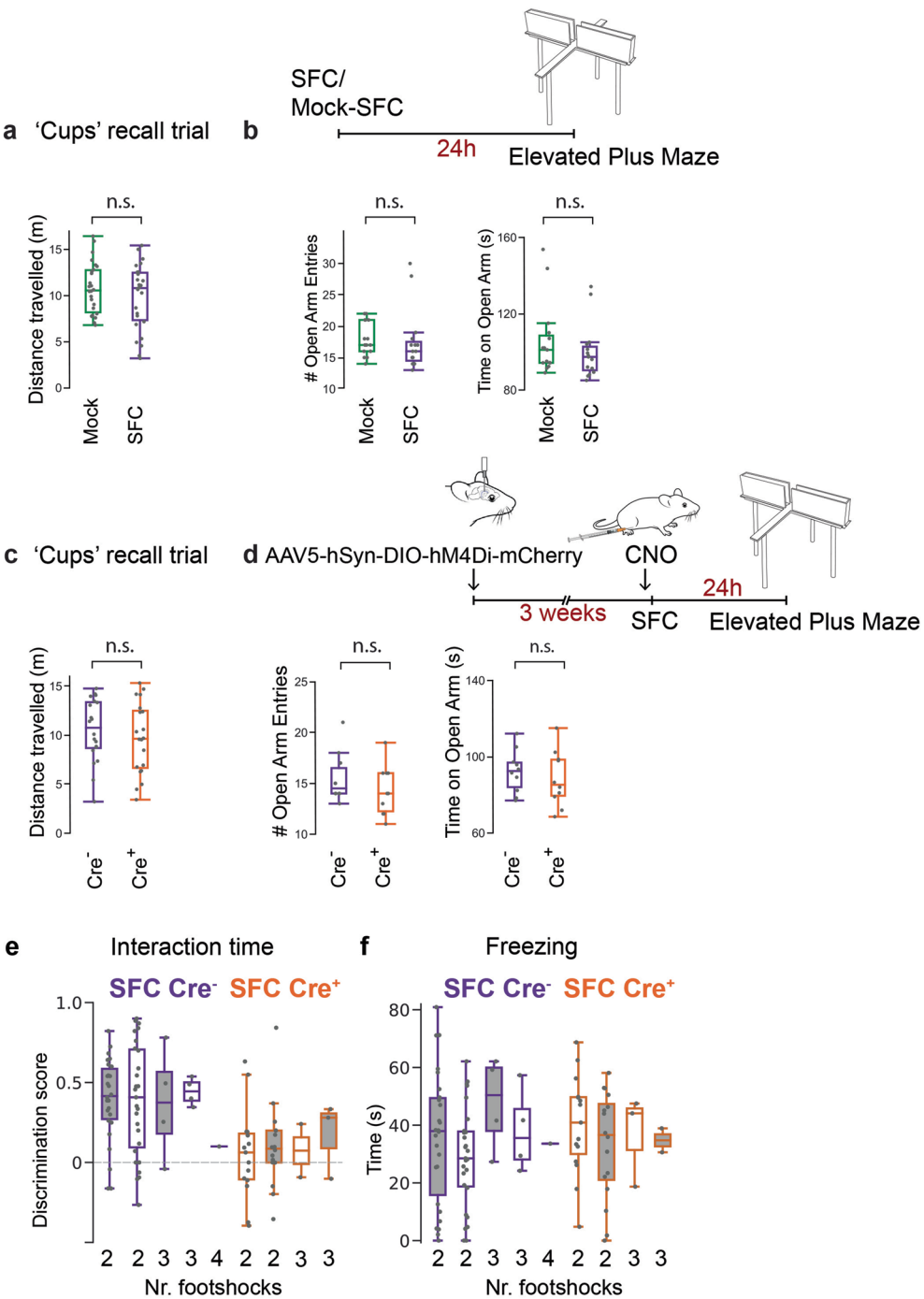

Extended Data Fig. 3 | See next page for caption.

https://doi.org/10.1038/s41593-024-01771-8

Extended Data Fig. 3 | General anxiety-like behavior and locomotor activity are not affected by SFC, and SFC behaviors do not depend on number of foot shocks administered. a, No difference in locomotion between mock-SFC and SFC cohorts as quantified by the distance traveled during the non-social 'cups' recall trial 24 h after SFC. Two-sided, unpaired *t*-test: Distance traveled t = 1.019, p = 0.313. N = 26 C57BL/6J wild-type mice per cohort. Data in **a** and **c** are from Figs. 2 and 3, respectively. **b**, No difference in general anxiety behaviors between mock-SFC and SFC cohorts as quantified with the elevated plus maze (EPM) 24 h after SFC. Two-sided, unpaired t-test: open arm entries t = 0.32, p = 0.751, time on open arm: t = 0.934, p = 0.358. N = 15 C57BL/6J wild-type mice per cohort. **c**, No difference in locomotion between SFC Cre$^-$ and Cre$^+$ cohorts with CNO injection 30 mins prior to the SFC session is observed for the distance traveled during the 'cups' recall trial 24 h after SFC. Two-sided, unpaired *t*-test: Distance traveled t = 0.767, p = 0.447. SFC Cre$^-$: N = 10 *Avpr1b-Cre*$^-$ and N = 10 *Amigo2-Cre*$^-$; SFC Cre$^+$: N = 10 *Avpr1b-Cre*$^+$ and N = 10 *Amigo2-Cr*$^+$. **d**, No difference in general anxiety between SFC Cre$^-$ and Cre$^+$ cohorts is observed during exploration of the EPM 24 h after SFC, with CNO administration 30 min prior to the EPM assay. Two-sided, unpaired t-test: open arm entries t = 1.092, p = 0.289, time on open arm: t = 0.637, p = 0.531. N = 10 *Amigo2-Cre*$^-$ and N = 10 *Amigo2-Cre*$^+$. **e**, Discrimination score based on CS$^-$ versus CS$^+$ interaction times (y-axis) as a function of number of foot shocks received by subject mouse during SFC (x-axis). Data are shown for SFC Cre$^-$ control mice (purple outlined boxes) and SFC Cre$^+$ mice (orange outlined boxes); both groups received CNO 30 min prior to SFC on day 1. Data for female mice (gray bars) and male mice (open bars) are shown separately. No difference between discrimination scores during social recall 24 h after SFC for Cre$^-$ mice receiving 2 versus 3 or 4 foot shocks (two-sided Welch's *t*-test: t = 0.213, p = 0.836) and for Cre$^+$ mice receiving 2 versus 3 foot shocks (two-sided Welch's *t*-test: t = −0.48, p = 0.643). **e**,**f**, SFC Cre$^-$: N = 31 *Avpr1b-Cre*$^-$ and N = 31 *Amigo2-Cre*$^-$ (N = 53 mice administered 2-foot shocks); SFC Cre$^+$: N = 18 *Avpr1b-Cre*$^+$ and N = 18 *Amigo2-Cre*$^+$; 31 mice administered 2-foot shocks). Sex is balanced per condition. **f**, No difference in freezing duration during social recall trial 24 h after SFC for Cre$^-$ mice receiving 2 versus 3 or 4 foot shocks (two-sided Welch's *t*-test: t = −1.71, p = 0.121). No difference in freezing duration during the social recall trial 24 h after SFC for Cre$^+$ mice receiving 2 versus 3 foot shocks (two-sided Welch's *t*-test: t = 0.08, p = 0.938). Box plots: central line, median; bottom and top edges, 25th and 75th percentiles; whiskers, most extreme data points (excluding outliers); dots, individual animals.

https://doi.org/10.1038/s41593-024-01771-8

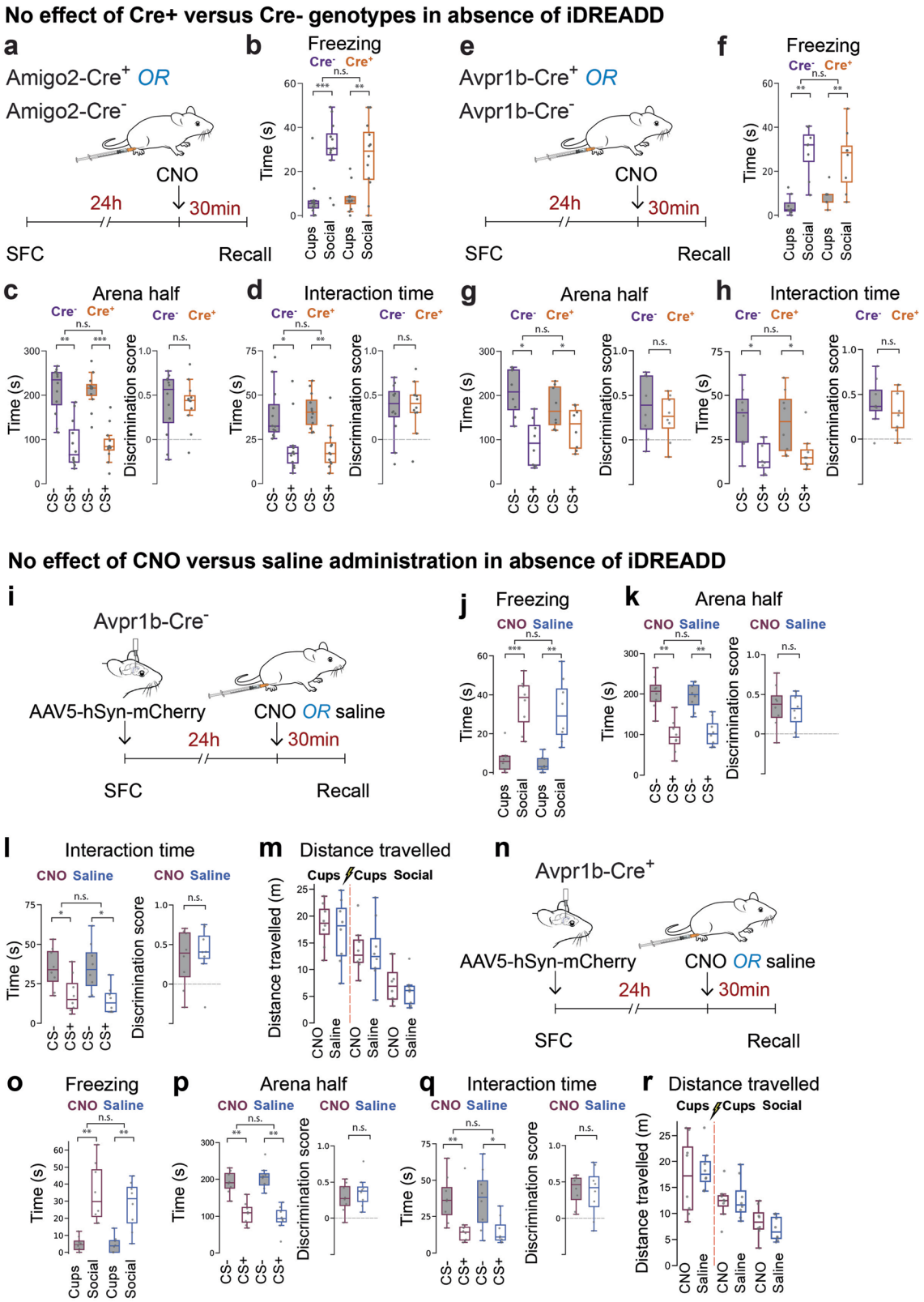

Extended Data Fig. 4 | See next page for caption.

https://doi.org/10.1038/s41593-024-01771-8

Extended Data Fig. 4 | No significant effect of Cre$^+$ genotype or CNO administration in absence of iDREADD expression. a, Cre$^-$ and Cre$^+$ littermates underwent SFC (day 1) and were intraperitoneally injected with CNO on day 2, 30 min prior to social recall. N = 12 *Amigo2-Cre*$^-$ and N = 12 *Amigo2-Cre*$^+$ mice in **a**–**d**. Sex is balanced per condition. **b**, *Amigo2-Cre*$^-$ and *Amigo2-Cre*$^+$ cohorts displayed similar freezing durations 24 h after SFC (two-way repeated measures ANOVA: genotype × stage, $F(1,44) = 0.871$, $p = 0.68$). **c**, Spent a comparable amount of time in the CS$^-$ versus CS$^+$ arena half (two-way ANOVA: genotype × arena half, $F(1,44) = 1.97$, $p = 0.52$; right, discrimination scores, two-sided unpaired *t*-test $t = -0.033$, $p = 0.973$). **d**, Displayed comparable CS$^-$ versus CS$^+$ interaction times (two-way ANOVA: genotype × stimulus mouse, $F(1,44) = 1.28$, $p = 0.47$; right, discrimination scores, two-sided unpaired *t*-test: $t = 0.292$, $p = 0.772$. **e**–**h**, Same paradigm as in **a**–**d** but with *Avpr1b-Cre*$^+$ and *Avpr1b-Cre*$^-$ subject mice. N = 8 *Avpr1b-Cre*$^+$, N = 8 *Avpr1b-Cre*$^-$ in **e**–**r**. Sex is balanced per condition. **f**, *Avpr1b-Cre*$^-$ and *Avpr1b-Cre*$^+$ cohorts displayed similar freezing duration 24 h after SFC (two-way repeated measures ANOVA: genotype × stage, $F(1,28) = 1.298$, $p = 0.26$) and **g**, spent comparable times in the CS$^-$ and the CS$^+$ arena halves, respectively (two-way ANOVA: genotype × arena half, $F(1,28) = 1.384$, $p = 0.24$; right, discrimination scores, two-sided unpaired *t*-test $t = -0.832$, $p = 0.41$) and **h**, displayed comparable CS$^-$ versus CS$^+$ interaction times (two-way ANOVA: genotype × stimulus mouse, $F(1,28) = 0.225$, $p = 0.638$). Right, discrimination scores, two-sided unpaired *t*-test: $t = -0.744$, $p = 0.46$. **i**, To assess whether effects of SFC differ between CNO-administered (fuchsia) versus saline-administered (blue) *Avpr1b-Cre*$^-$ mice, both cohorts expressed mCherry in dCA2 and underwent SFC on experimental day 1. Twenty-four hours later, mice were intraperitoneally injected with CNO or saline 30 min prior to recall. **j**–**m**: N = 8 *Avpr1b-Cre*$^-$ mice per condition (CNO or saline). Sex is balanced per condition. **j**, CNO- and saline-administered *Avpr1b-Cre*$^-$ cohorts displayed similar freezing durations 24 h after SFC (two-way repeated measures ANOVA: treatment (saline or CNO) × stage, $F(1,28) = 0.029$, $p = 0.865$), (**k**) spent comparable times in the CS$^-$ and the CS$^+$ arena halves (two-way ANOVA: treatment × arena half, $F(1,28) = 4.468$, $p = 0.051$; right, discrimination scores, two-sided, unpaired *t*-test $t = -0.47$, $p = 0.643$), (**l**) displayed comparable CS$^-$ versus CS$^+$ interaction times (two-way ANOVA: treatment × stimulus mouse, $F(1,28) = 0.243$, $p = 0.625$; right, discrimination scores, two-sided unpaired *t*-test: $t = 0.427$, $p = 0.676$) and (**m**) traveled comparable distances (two-way repeated measures ANOVA: cohort × stage, $F(2,42) = 0.077$, $p = 0.925$). **n**, As in **i**–**m**, with CNO- or saline-administered *Avpr1b-Cre*$^+$ cohorts. **o**–**r**: N = 8 *Avpr1b-Cre*$^+$ mice per condition (CNO or saline). Sex is balanced per condition. **o**, CNO- and saline-administered *Avpr1b-Cre*$^+$ cohorts displayed similar freezing durations 24 h after SFC (two-way repeated measures ANOVA: treatment × stage, $F(1,28) = 0.676$, $p = 0.417$), (**p**) spent comparable times in the CS$^-$ and the CS$^+$ arena halves (two-way ANOVA: treatment × arena half, $F(1,28) = 1.374$, $p = 0.251$; right, discrimination scores, two-sided unpaired *t*-test $t = 0.828$, $p = 0.42$), (**q**) displayed comparable CS$^-$ versus CS$^+$ interaction times (two-way ANOVA: treatment × stimulus mouse, $F(1,28) = 0.074$, $p = 0.786$; right, discrimination scores, two-sided unpaired *t*-test: $t = -0.185$, $p = 0.855$) and (**r**) traveled comparable distances (two-way repeated measures ANOVA: cohort × stage, $F(2,42) = 0.391$, $p = 0.678$). Bonferroni post hoc tests: $^*p < 0.05$, $^{**}p < 0.01$, $^{***}p < 0.001$. Box plots: central line, median; bottom and top edges, 25th and 75th percentiles; whiskers, most extreme data points (excluding outliers); dots, individual animals.

https://doi.org/10.1038/s41593-024-01771-8

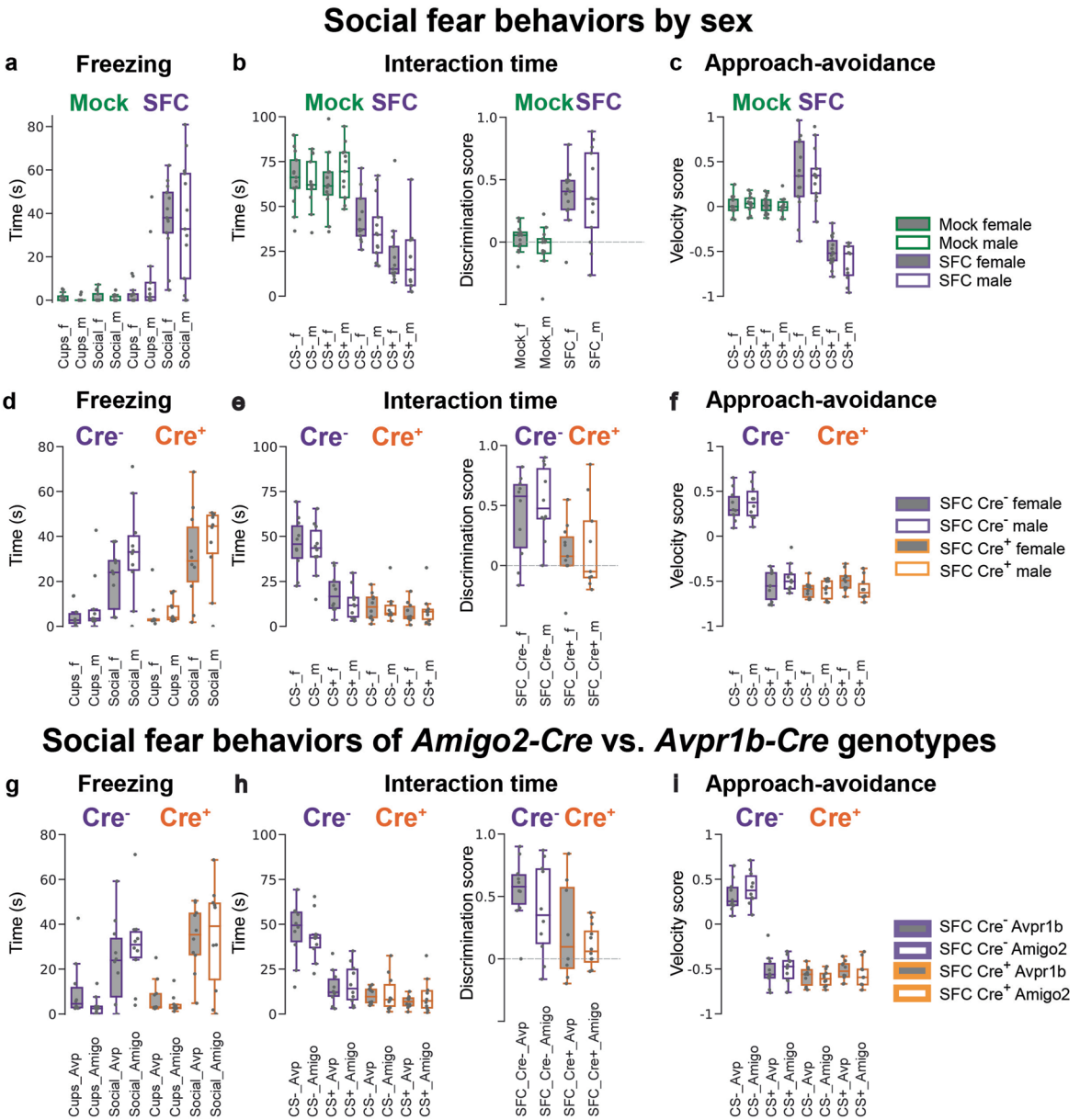

Extended Data Fig. 5 | No significant effect of sex or *Amigo2-Cre* versus *Avpr1b-Cre* genotype on SFC behaviors. a, No significant differences between female (gray fill) and male (white fill) mice with respect to freezing duration during the non-social 'cups' and the 'social' recall trials 24 h after mock-SFC (green outline) or 24 h after SFC (purple outline; three-way repeated measures ANOVA: cohort × sex × stage, $F(1,96) = 0.69$, $p = 0.4$). Data in **a**–**c** are from Fig. 2a,b–f: N = 26 C57BL/6J wild-type mice per experimental condition. Sex is balanced per condition. **b**, Female and male mock-SFC and SFC mice spend a comparable amount of time interacting with the CS^- and the CS^+ stimulus mouse, with no significant difference between sexes (three-way repeated measures ANOVA: cohort × sex × stimulus mouse, $F(1,96) = 0.14$, $p = 0.7$). Right, discrimination scores, two-way ANOVA: cohort × sex, $F(1,48) = 0.227$, $p = 0.6357$. **c**, There is no significant difference between female and male mock-SFC and SFC mice in their relative velocities of approach versus retreat toward the CS^- and the CS^+ stimulus mice. Velocity score = (approach velocity − retreat velocity)/sum of velocities, (three-way repeated measures ANOVA: cohort × sex × arena half, $F(1,96) = 0.8$, $p = 0.37$). **d**, Female and male mice display similar freezing durations during the non-social 'cups' recall trial and the 'social' recall trial 24 h after SFC, for both Cre^- control (purple) and Cre^+ cohorts (orange; three-way repeated measures ANOVA: cohort × sex × stage, $F(1,72) = 0.064$, $p = 0.8$). Data in **d**–**i** are from Fig. 2g–l; SFC Cre^-: N = 10 *Avpr1b-Cre*$^-$, N = 10 *Amigo2-Cre*$^-$, SFC Cre^+: N = 10 *Avpr1b-Cre*$^+$, N = 10 *Amigo2-Cre*$^+$. Sex is balanced per condition. **e**, No significant differences between female and male Cre^- and Cre^+ mice with respect to social interaction times with the CS^- and the CS^+ stimulus mouse (three-way repeated measures ANOVA: cohort × sex × stimulus mouse, $F(1,72) = 0.341$, $p = 0.56$). Right, discrimination scores (two-way ANOVA: cohort × sex, $F(1,36) = 0.577$, $p = 0.452$). **f**, Female and male Cre^- and Cre^+ mice display comparable relative velocities of approach versus retreat toward the CS^- and the CS^+ stimulus mouse (three-way repeated measures ANOVA: cohort × sex × arena half, $F(1,72) = 1.15$, $p = 0.29$). **g**, No significant differences between Cre^- (purple) or Cre^+ (orange) *Avpr1b-Cre* and *Amigo2-Cre* mice with respect to freezing duration for the non-social 'cups' recall trial and the 'social' recall trial 24 h after SFC (three-way repeated measures ANOVA: cohort (Cre^- vs. Cre^+) × genotype (Amigo2- vs. Avpr1b-Cre) × stage, $F(1,72) = 0.615$, $p = 0.44$). **h**, No significant differences between *Avpr1b-Cre* and *Amigo2-Cre* Cre^- or Cre^+ mice with respect to social interaction time and no significant difference between sexes (three-way repeated measures ANOVA: cohort × genotype × stimulus mouse, $F(1,72) = 0.165$, $p = 0.685$). Right, discrimination scores, two-way ANOVA: cohort × genotype, $F(1,36) = 0.004$, $p = 0.95$. **i**, No significant differences between *Avpr1b-Cre* and *Amigo2-Cre* Cre^- and SFC Cre^+ mice for relative approach/retreat velocities (three-way repeated measures ANOVA: cohort × genotype × arena half, $F(1,72) = 0.08$, $p = 0.7758$). Box plots: central line, median; bottom and top edges, 25th and 75th percentiles; whiskers, most extreme data points (excluding outliers); Dots, individual animals.

https://doi.org/10.1038/s41593-024-01771-8

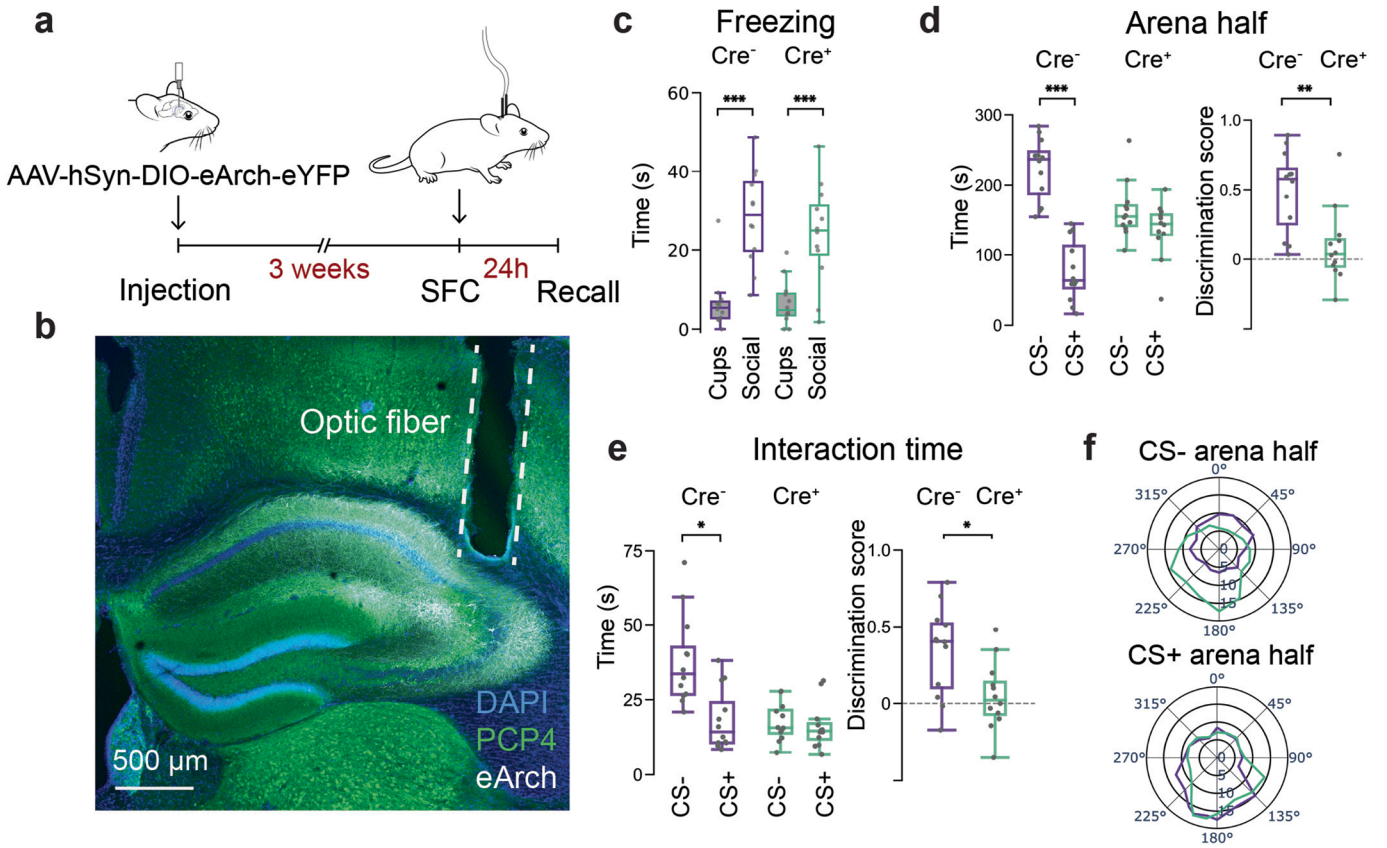

Extended Data Fig. 6 | Optogenetic silencing of dCA2 during SFC disrupts social fear discrimination memory. a, An optogenetic approach was used during SFC on day 1 to silence dCA2 selectively during social fear memory encoding: Cre^+ mice and Cre^- littermates were injected in dCA2 with AAV-DIO-eArch3.0-eYFP and implanted with bilateral ferrules for optic fiber probes above dCA2. dCA2 was illuminated in Cre^+ and Cre^- groups with green light pulses continually during the 5-min SFC learning trial. **b**–**f**: N = 12 *Amigo2-Cre*$^-$ (purple) mice; N = 12 Amigo2-Cre+(turquoise). Sex is balanced per condition. **b**, Example confocal image from an *Amigo2-Cre*$^+$ mouse showing optical fiber tract (dashed lines) and eArch3 expression with co-expression of the CA2 marker protein PCP4. **c**, SFC Cre^+ and Cre^- cohorts display similar freezing duration during recall trials 24 h after SFC (two-way repeated measures ANOVA: cohort × stage, $F(1,40) = 0.75$, $p = 0.72$) and significantly elevated freezing levels during the 'social' as compared to the 'cups' recall trial (Bonferroni post hoc tests). **d**, Cre^- cohorts show a preference for exploring the arena half containing the CS^- mouse, whereas Cre^+ cohorts show generalized avoidance of the CS^+ and the CS^- arena halves (two-way repeated measures ANOVA: cohort × arena half, $F(1, 40) = 8.219$, $p = 6.58 \times 10^{-3}$). Right, discrimination scores: unpaired, two-sided *t*-test between cohorts: $t = -3.256$, $p = 0.003$. **e**, Cre^- cohorts prefer to interact with the CS^- mouse, whereas Cre^+ mice display generalized avoidance toward the CS^+ and CS^- mice (two-way repeated measures ANOVA: cohort × stimulus mouse, $F(1,40) = 7.429$, $p = 9.47 \times 10^{-3}$). Right, discrimination scores: unpaired two-sided *t*-test between cohorts: $t = 2.791$, $p = 0.01$. **f**, Velocity per head orientation angle plot, illustrating the generalized avoidance behaviors of dCA2-silenced Cre^+ mice (turquoise) but not of Cre^- controls which maintain selective approach-avoidance toward the CS^- mouse (purple). Bonferroni post hoc and *t*-tests, as appropriate: *p < 0.05, **p < 0.01, ***p < 0.001. n.s.: not significant. Box plots: central line, median; bottom and top edges, 25th and 75th percentiles; whiskers, most extreme data points (excluding outliers); dots, individual animals.

https://doi.org/10.1038/s41593-024-01771-8

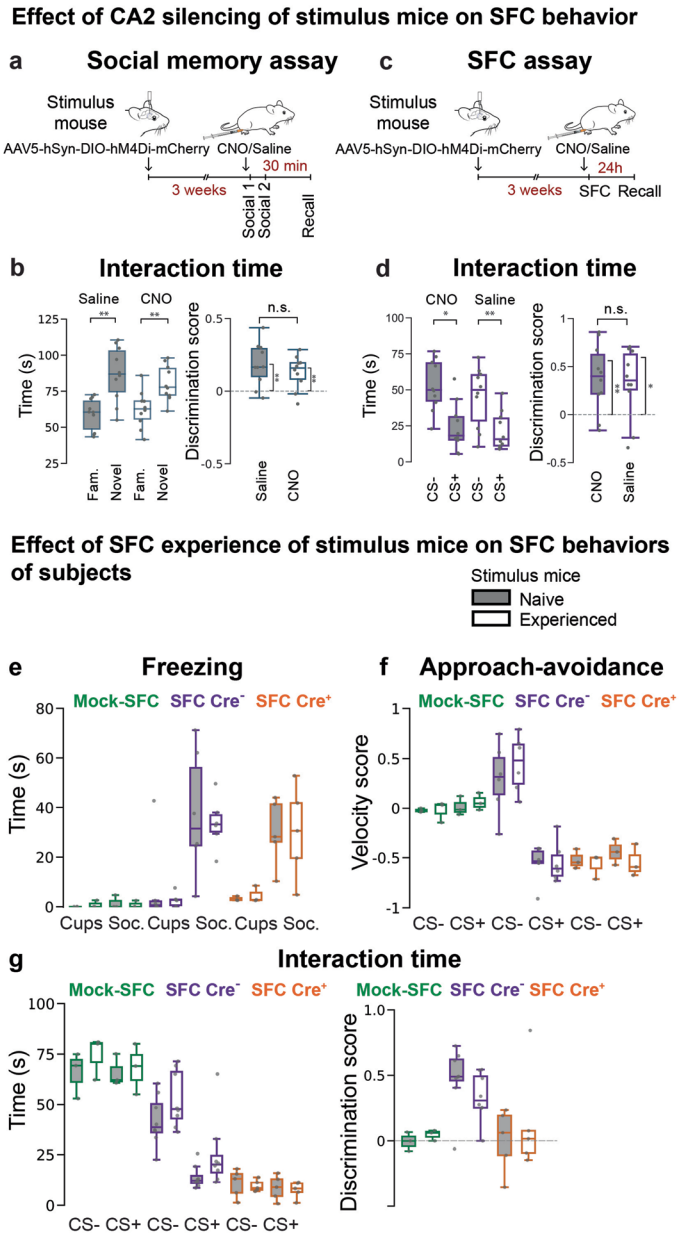

Extended Data Fig. 7 | See next page for caption.

https://doi.org/10.1038/s41593-024-01771-8

Extended Data Fig. 7 | Stimulus mouse experience does not affect social memory or social fear discrimination memory in subject mice. a,**b**, Social memory assay with dCA2-silenced male *Amigo2-Cre* stimulus mice. **a**, After 3–4 weeks of iDREADD injections, CNO was administered to stimulus mice 30 min prior to the first social memory encoding session ('social 1'), which was immediately followed by a second encoding session ('social 2') with the position of stimulus mice swapped. Thirty minutes later, a stimulus mouse, chosen at random, was replaced by a novel mouse ('recall'). One week later (week 2), the procedure is repeated with saline injection administered to the same stimulus mice and a new cohort of subject mice. This was repeated with a different pair of stimulus mice and two cohorts of subject mice, resulting in a total of N = 20 C57BL/6J wild-type male subject mice (N = 5 per cohort). **b**, Left, subject mice display comparable interaction times when stimulus mice were administered CNO versus saline, two-way ANOVA: injection type × stimulus mouse (novel or familiar), $F(1,36) = 1.14$, $p = 0.293$. Right, discrimination scores; unpaired, two-sided *t*-test: $t = -0.879$, $p = 0.39$). One-sided, one-sample *t*-tests against zero: stimulus mouse + saline, $p = 0.0057$, $t = 3.603$; stimulus mouse + CNO, $t = 3.882$, $p = 0.0037$. **c**,**d**, SFC assay with dCA2-silenced male *Amigo2-Cre* stimulus mice. **c**, After 3–4 weeks of iDREADD injections, CS^+ and CS^- stimulus mice received CNO 30 min before SFC. The same stimulus mice were used for SFC 1 week later with saline injections and a new cohort of subject mice. This was repeated with a different pair of stimulus mice and two different cohorts of subject mice, resulting in a total of N = 20 male subject mice (N = 5 per cohort). **d**, Left, subject mice display comparable interaction times toward CNO- versus saline-administered CS^+ versus CS^- stimulus mice. Two-way ANOVA: injection type × stimulus mouse (CS^+ or CS^-), $F(1,36) = 0.98$, $p = 0.328$. Right, discrimination scores; unpaired, two-sided *t*-test: $t = 0.342$, $p = 0.736$. One-sided, one-sample *t*-tests against zero: stimulus mouse + saline, $t = 2.806$, $p = 0.02$; Stimulus mouse + CNO, $t = 3.403$, $p = 0.007$. Bonferroni post hoc tests: *p < 0.05, ** p < 0.01. **e**–**g**, Effect of prior SFC experience by CS^+ and CS^- stimulus mice on subject mouse behavior for mock-SFC (green; N = 6 C57BL/6J wild-type mice per condition), SFC Cre^- (purple; N = 3 *Avpr1b-Cre*$^-$, N = 3 *Amigo2-Cre*$^-$ per condition) or SFC Cre^+ (orange; N = 3 *Avpr1b-Cre*$^+$, N = 3 *Amigo2-Cre*$^+$ per condition) subject mice during recall trial on day 2. Sex is balanced per condition. **e**, Freezing duration of mock-SFC (green), SFC Cre^- (purple) or SFC Cre^+ (orange) subject mice during recall trial on day 2 does not significantly differ when stimulus mice are 'naive' (gray-filled bars; no prior SFC experience) versus 'experienced' (open bars; used in prior SFC experiments with N = 5 subjects; three-way repeated measures ANOVA: cohort × stage × stim. mouse experience, $F(2,40) = 0.016$, $p = 0.984$). **f**, No significant difference in relative velocities toward naive or experienced CS^- or CS^+ mice, three-way ANOVA: cohort × arena half × stim. mouse experience, $F(2,40) = 0.2$, $p = 0.82$. **g**, Comparable interaction times of subjects with naive versus experienced stimulus mice (three-way repeated measures ANOVA: cohort × stimulus mouse (CS^- vs. CS^+) × stim. mouse experience, $F(2,40) = 0.126$, $p = 0.88$). Right, discrimination scores, two-way ANOVA: cohort × stim. mouse experience, $F(2,20) = 1.04$, $p = 0.37$. Data pooled from Figs. 2 and 3 and Extended Data Fig. 2a,b, with corresponding sex and genotype. Box plots: central line, median; bottom and top edges, 25th and 75th percentiles; whiskers, most extreme data points (excluding outliers); dots, individual animals. Bonferroni post hoc and *t*-tests, as appropriate: *p < 0.05, **p < 0.01. n.s.: not significant.

https://doi.org/10.1038/s41593-024-01771-8

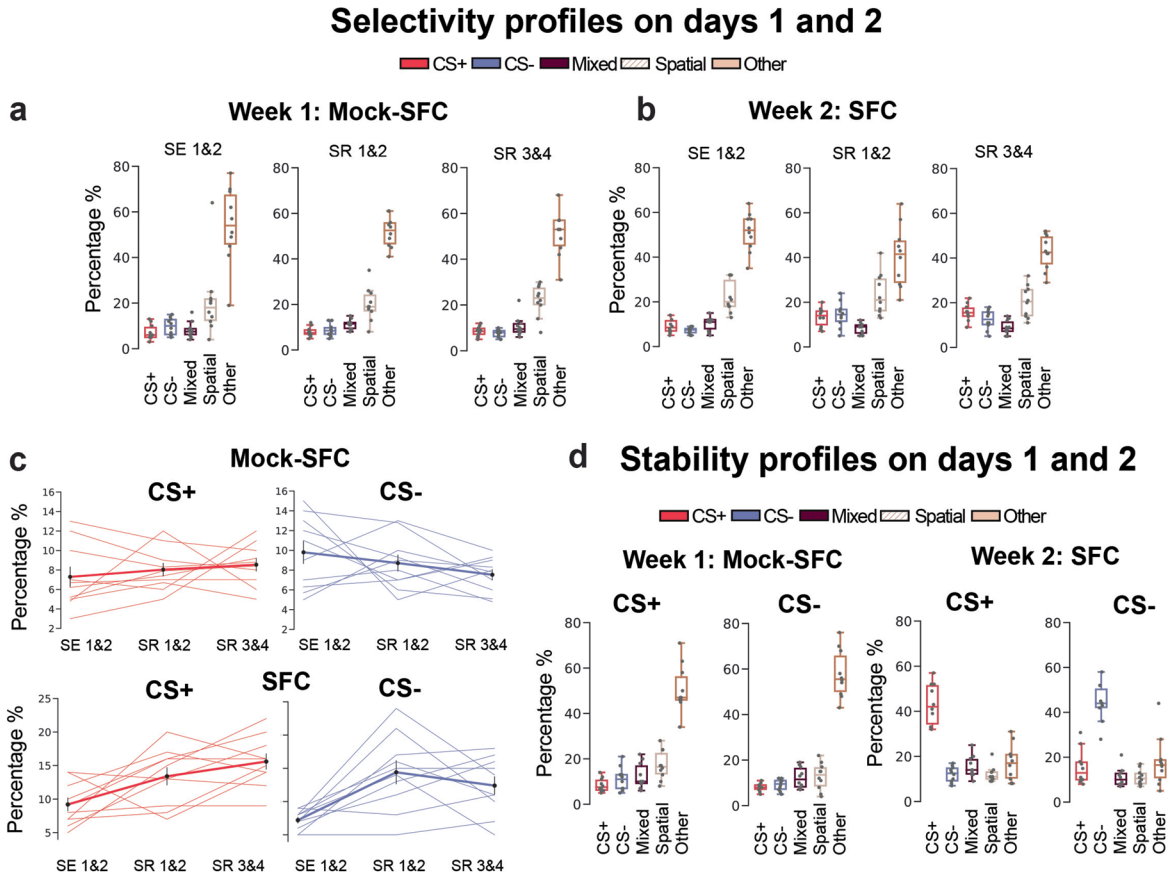

Extended Data Fig. 8 | Comparison of dCA2 neuron stimulus selectivity and stability before and after mock-SFC and SFC for individual mice. a, No change in the CS^- or CS^+ selective fraction of cells was observed across mock-SFC (two-sided $\chi^2(6) = 4.943$, $p = 0.551$). Dots, individual mice. SE: social exploration trials before mock-SFC; SR: social recall trials after mock-SFC. Data corresponding to Fig. 5e. **a**–**d**: N = 5 male *Amigo2-Cre*$^+$ and 5 male *Avpr1b-Cre*$^+$ mice. **b**, SFC significantly increased the fraction of cells that responded selectively to the CS^+ or the CS^- (chi-square test; two-sided $\chi^2(6) = 34.382$, $p = 5.675 \times 10^{-6}$). Dots, individual mice. Data corresponding to Fig. 5e. SE: social exploration trials before SFC; SR: social recall trials after SFC. **c**, Percentage of CS^+ (left) and CS^- (right) selective dCA2 pyramidal neurons (y-axis; see **a** and **b**), plotted as a function of social exploration or social recall trials (x-axis): for mock-SFC (top) and SFC cohorts (bottom). Mock-SFC: one-way repeated measures ANOVA CS^+: $F(2,18) = 0.68$, $p = 0.519$; CS^-: $F(2,18) = 1.497$, $p = 0.2503$. SFC: one-way repeated measures ANOVA CS^+: $F(2,18) = 7.177$, $p = 0.00512$; CS^-: $F(2,18) = 8.996$, $p = 0.00195$. Thin lines: individual animals. Filled symbols connected by thick lines and error bars in **a** and **c**: mean ± SEM averaged across animals. Data are from Fig. 5e. **d**, Individual animal data showing the stability of dCA2 neuron response profiles for cells that initially responded on day 1 selectively to CS^+ or CS^- (labeled above graphs) before mock-SFC (left) or SFC (right). Graphs show response profiles for CS^+ and CS^- selective cells identified on day 1 when measured during the recall trial on day 2 after mock-SFC or SFC. For the SFC cohort, cells selective for the CS^+ or CS^- on day 1 show a greater probability of responding, respectively, to the CS^+ or the CS^- in the recall trial after SFC (day 2). Data are from Fig. 5h. Total number of cells (mean ± SEM across mice): mock-SFC day 1: 672 (69 ± 14); mock-SFC day 2: 658 (64 ± 10); SFC day 1: 647 (62 ± 7); SFC day 2: 630 (58 ± 6). Cells that responded to both CS^+ and CS^- were classified as 'mixed selective'. Box plots: central line, median; bottom and top edges, 25th and 75th percentiles; whiskers, most extreme data points (excluding outliers); dots, individual animals.

https://doi.org/10.1038/s41593-024-01771-8

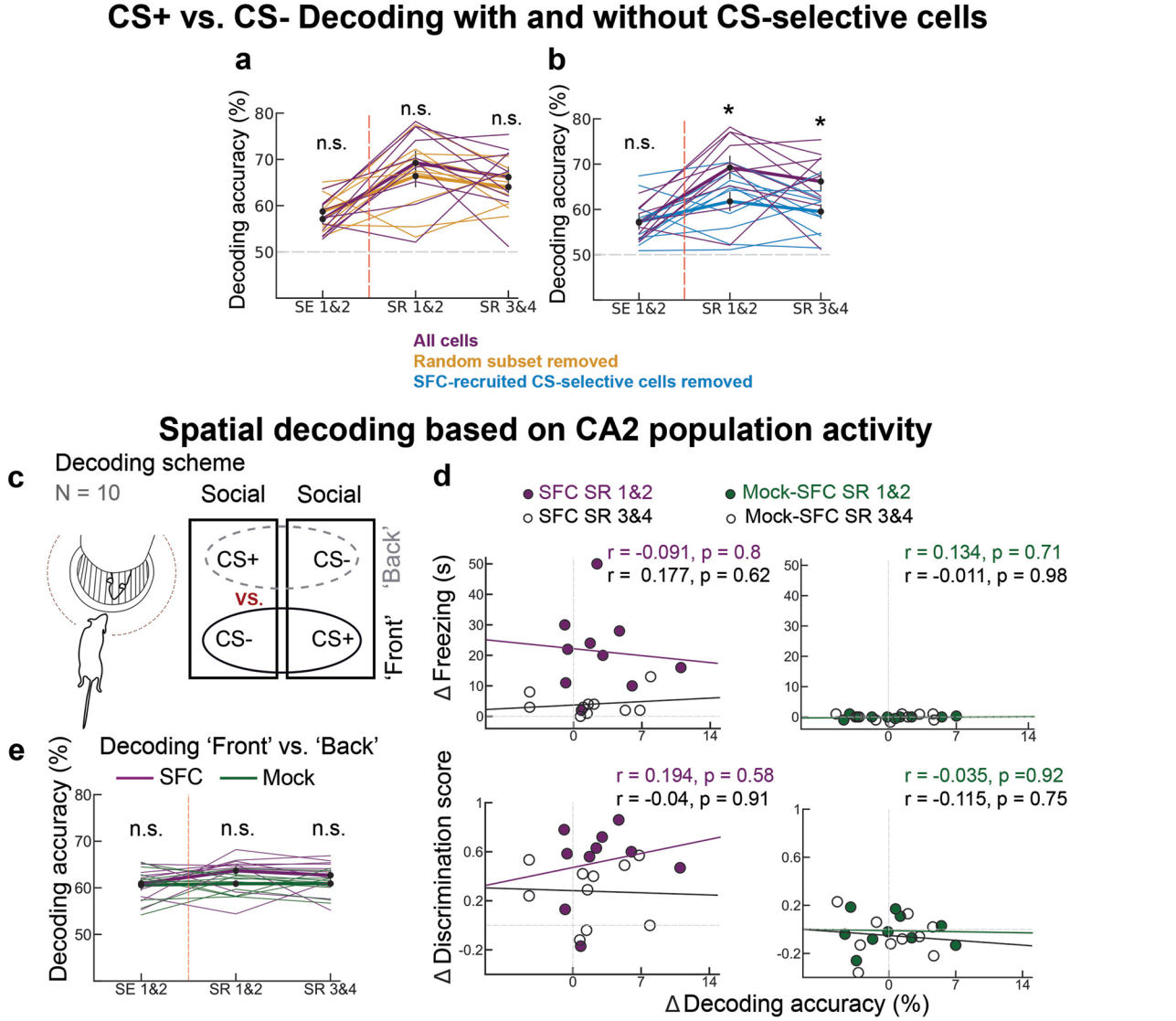

Extended Data Fig. 9 | CS-selective cells enhance identity decoding after SFC, but spatial decoding performance is not enhanced after SFC. a, CS^+ versus CS^- decoding accuracies for two social exploration trials (SE) on day 1 before SFC and social recall trials on day 2 after SFC (SR 1 and 2; SR 3 and 4). Decoding is based on the original dataset (purple; Fig. 6) or when a randomly selected subset of 11% of cells were removed from (ochre). Thin lines show individual animals; circles and thick lines show mean ± SEM. Decoding accuracies for the two datasets are comparable throughout the experiment: two-way repeated measures ANOVA: cohort × session, $F(2,54) = 0.018$, $p = 0.98$. For both datasets, decoding of CS^+ versus CS^- is significantly greater after SFC (one-sided, paired *t*-tests: all cells SR12 vs. SE12: $t = -4.42$, $p = 0.00083$; random subset removed SR12 vs. SE12: $t = -2.82$, $p = 0.01$). **a**–**e**: N = 5 male *Amigo2-Cre*$^+$ and 5 male *Avpr1b-Cre*$^+$ mice per cohort. **b**, Decoding based on the original dataset (purple ; Fig. 6) or with the 11% of CS^+ and CS^- selective cells newly recruited after SFC was removed from the population for all time points (blue). Removal of the newly recruited selective cells caused a significant decrease in decoding accuracy after SFC but not before SFC. Decoding accuracies for the two datasets are significantly different for the different SFC stages (two-way repeated measures ANOVA: cohort × session, $F(2,54) = 3.623$, $p = 0.0334$). When CS^+ and CS^- selective cells newly recruited by SFC have been removed, no enhancement of decoding accuracy can be observed (one-sided, paired *t*-tests, CS-selective cells removed SR12 vs. SE12: $t = -1.81$, $p = 0.051$). Bonferroni post hoc tests: *$p < 0.05$, n.s.: not significant. Decoding accuracy, mean ± SEM: all cells (purple; SE 1 and 2: 57.1 ± 1.15, SR 1 and 2: 69.24 ± 2.62, SR 3 and 4: 66.17 ± 2.25); random subset (11% cells) removed (ochre; SE 1 and 2: 58.74 ± 1.32, SR 1 and 2: 66.39 ± 2.42, SR 3 and 4: 64.03 ± 1.3); SFC-recruited CS^+ and CS^- selective cells removed (blue; SE 1 and 2: 57.27 ± 1.76, SR 1 and 2: 61.76 ± 2.13, SR 3 and 4: 59.53 ± 1.6). Unpaired, two-sided *t*-test, comparison of decoding accuracies when random subset removed versus when CS^+ and CS^- selective cells removed for SR 1 and 2: $t = -2.34$, $p = 0.031$. Thin lines show individual animals; circles and thick lines show mean ± SEM. **c**, To assess how SFC impacts dCA2 representations of spatial variables, dCA2 calcium activity data were acquired during social–spatial interactions with the CS^+ and CS^- in front and back right cups before and after SFC. Arena and spatial location of cups differ from SFC learning trial so only social information is present in the recall trial relevant to SFC. dCA2 activity data were pooled from interactions around the same cup location (i.e., back or front cup) from two consecutive recall trials, irrespective of stimulus mouse identity. **d**, r, Pearson's correlation coefficient. Changes in spatial decoding are not correlated with changes in freezing behavior (top graphs) or behavioral discrimination of CS^+ from CS^- (bottom graphs) for SFC (left graphs) or mock-SFC cohorts (right graphs). **e**, Spatial decoding accuracy is similar before (SE trial) and after (SR trials) SFC (purple). SFC and mock-SFC (green) cohorts show similar spatial decoding accuracy throughout the paradigm, suggesting that the past threat-associated experience associated with a conspecific does not affect the representation of position in the recall arena. Two-way ANOVA: cohort × session, $F(2,54) = 1.284$, $p = 0.285$. Bonferroni post hoc tests: n.s.: not significant. Thin lines show individual animals; circles and thick lines show mean ± SEM.

https://doi.org/10.1038/s41593-024-01771-8

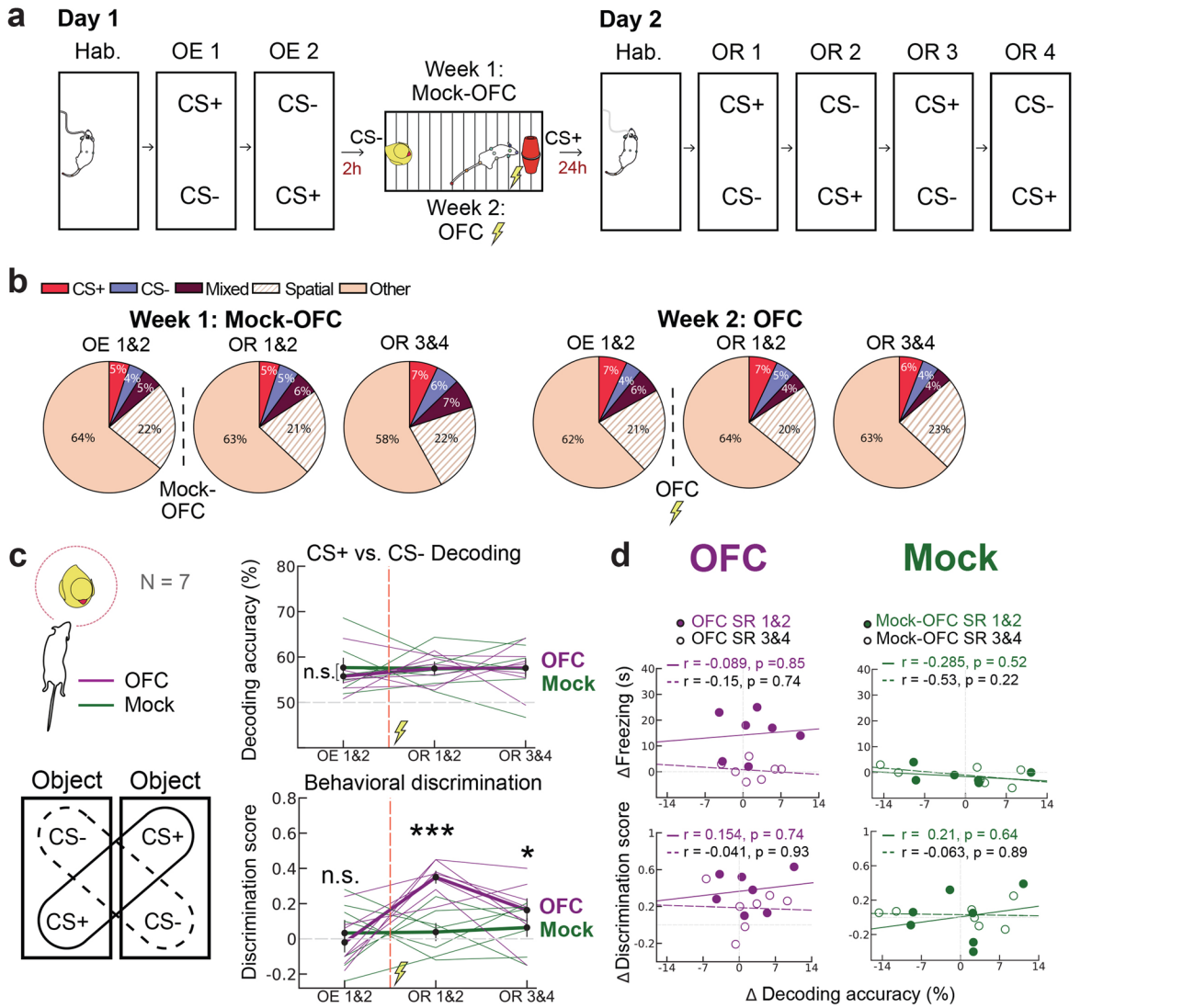

Extended Data Fig. 10 | OFC does not enhance dCA2 single-cell or population-level responses to safety- versus threat-associated objects. a, OFC paradigm. On day 1, a subject mouse was allowed to explore an open arena (the same used for SFC social exploration and recall trials) for 5 min ('Hab.'), followed by two 5-min trials in which the subject explored the prospective CS^+ and CS^- objects (OE, 'object exploration' trials), with positions swapped across trials. In week 1, OE trials were followed 2 hours later by a mock-OFC trial. On day 2, the subject was re-exposed to the open arena ('Hab.'), followed by four consecutive 'object recall' (OR) trials, with positions of stimulus objects swapped between each trial. In week 2, the same procedure was repeated with two novel objects and with the mock-OFC trial replaced by an OFC trial. **b**, dCA2 cells with indicated response selectivity profiles; cells that responded to both CS^+ and CS^- objects were classified as 'mixed selective'. **b**–**d**, N = 7 mice (N = 3 male *Amigo2-Cre*$^+$; N = 4 male *Avpr1b-Cre*$^+$ mice). OFC did not significantly change the fraction of CS^+ or CS^- selective, mixed-selective or spatially selective cells (two-sided Chi-square tests; $\chi^2(6) = 6.26$, p = 0.395), no change of the responsive cell populations was observed for the mock-SFC cohort (two-sided $\chi^2(6) = 3.678$, p = 0.72). **c**, OFC did not alter population-level decoding of CS^+ versus CS^- objects. Top left, calcium activity was measured from dCA2 pyramidal neurons during exploration of CS^+ and CS^- objects in two object exploration (OE) trials on day 1 and four object recall (OR) trials on day 2 (after mock-OFC or OFC), with positions of objects swapped after each trial. Bottom left, linear SVM decoding of CS^+ versus CS^- objects from calcium data recorded with object positions swapped across two successive trials. Right graphs: top, CS^+ versus CS^- object decoding accuracy during two object exploration trials (OE) before OFC (purple) or before mock-OFC (green) and during the first two or the second two object recall trials (OR 1 and 2; OR 3 and 4) 24 h after OFC (purple) or 24 h after mock-OFC (green). Thin lines show individual animals; circles and thick lines are mean ± SEM. Bottom, behavioral discrimination scores before and after OFC and mock-OFC (averaged across two consecutive trials). OFC enhances behavioral discrimination performance but not dCA2-based decoding accuracy of objects (two-way repeated measures ANOVA: cohort × session, $F(2,36) = 0.1933$, p = 0.825 for decoding and $F(2,36) = 5.017$, p = 0.0119 for behavior). Paired, one-sided *t*-test against chance-level accuracies from null model. Bonferroni post hoc and *t*-tests, as appropriate: *p < 0.05, ***p < 0.001, n.s.: not significant. **d**, r, Pearson's correlation coefficient. Changes in freezing behavior (top graphs) and behavioral discrimination of CS^+ from CS^- objects (bottom graphs) plotted versus change in decoding accuracy of CS^+ from CS^- objects after OFC (left graphs; purple) or mock-OFC (right graphs; green) relative to values before OFC or mock-OFC. Filled symbols and solid lines; data from OR1 and OR2 recall trials; open symbols and dashed lines, data from OR3 and OR4 recall trials. No significant correlation between behavior and decoding performance. Circles represent individual animals. All mice were administered 2-foot shocks during OFC. Total number of cells (mean ± SEM per mouse): mock-OFC—object exploration trial, n = 456 cells (65 ± 11 per animal); object recall trial, n = 418 (64 ± 9 per animal); OFC—object exploration trials, n = 402 (57 ± 8 per animal); OFC object recall trials, n = 388 (55 ± 8 per animal).

nature portfolio

Corresponding author(s): Pegah Kassraian

Last updated by author(s): Jul 23, 2024

Reporting Summary

Nature Portfolio wishes to improve the reproducibility of the work that we publish. This form provides structure for consistency and transparency in reporting. For further information on Nature Portfolio policies, see our Editorial Policies and the Editorial Policy Checklist.

Statistics

For all statistical analyses, confirm that the following items are present in the figure legend, table legend, main text, or Methods section.

n/a	Confirmed
☐	☒ The exact sample size (*n*) for each experimental group/condition, given as a discrete number and unit of measurement
☐	☒ A statement on whether measurements were taken from distinct samples or whether the same sample was measured repeatedly
☐	☒ The statistical test(s) used AND whether they are one- or two-sided *Only common tests should be described solely by name; describe more complex techniques in the Methods section.*
☒	☐ A description of all covariates tested
☒	☐ A description of any assumptions or corrections, such as tests of normality and adjustment for multiple comparisons
☐	☒ A full description of the statistical parameters including central tendency (e.g. means) or other basic estimates (e.g. regression coefficient) AND variation (e.g. standard deviation) or associated estimates of uncertainty (e.g. confidence intervals)
☐	☒ For null hypothesis testing, the test statistic (e.g. *F*, *t*, *r*) with confidence intervals, effect sizes, degrees of freedom and *P* value noted *Give P values as exact values whenever suitable.*
☒	☐ For Bayesian analysis, information on the choice of priors and Markov chain Monte Carlo settings
☒	☐ For hierarchical and complex designs, identification of the appropriate level for tests and full reporting of outcomes
☒	☐ Estimates of effect sizes (e.g. Cohen's *d*, Pearson's *r*), indicating how they were calculated

Our web collection on statistics for biologists contains articles on many of the points above.

Software and code

Policy information about availability of computer code

Data collection	Data were collected using commercially available software reported in the Methods. Calcium recordings were acquired with Inscopix hard- and software, and behavioural tracking was performed using DeepLabCut.
Data analysis	Data were analyzed using commercially available, open source, and custom Python scripts. Detailed descriptions of these analyses are found in the Methods. We used Python (v.3.11.1) and the following python packages: 'os' (Version 2.1.4), 'sys' (Version 3.11.4) and 'utils' (Version 1.0.2) for system administration; 'numpy' (Version 2.0), 'scipy' (Version 1.14.0) and 'pandas' (Version 2.2.2) for data processing, data analysis and general data handling; 'scikit-learn' (Version 1.5.0) for preprocessing of the data for classification and k-means clustering; 'TensorFlow' (Version 2.11) and 'libsvm' (Version 3.23.0.4) for LSTM and Support Vector Machine classification respectively; 'Matplotlib' (Version 3.9), 'seaborn' (Version v0.11.2) and 'plotly' (Version 5.7) for data visualization.

For manuscripts utilizing custom algorithms or software that are central to the research but not yet described in published literature, software must be made available to editors and reviewers. We strongly encourage code deposition in a community repository (e.g. GitHub). See the Nature Portfolio guidelines for submitting code & software for further information.

Data

Policy information about availability of data

All manuscripts must include a data availability statement. This statement should provide the following information, where applicable:

- Accession codes, unique identifiers, or web links for publicly available datasets
- A description of any restrictions on data availability
- For clinical datasets or third party data, please ensure that the statement adheres to our policy

Datasets generated in the current study will be made available upon reasonable request. Source data are provided with this paper. Python code for underlying visualization and analysis can be obtained from https://github.com/Siegelbaumlab/dCA2_SFC

Human research participants

Policy information about studies involving human research participants and Sex and Gender in Research.

Reporting on sex and gender	N/A
Population characteristics	N/A
Recruitment	N/A
Ethics oversight	N/A

Note that full information on the approval of the study protocol must also be provided in the manuscript.

Field-specific reporting

Please select the one below that is the best fit for your research. If you are not sure, read the appropriate sections before making your selection.

☒ Life sciences ☐ Behavioural & social sciences ☐ Ecological, evolutionary & environmental sciences

For a reference copy of the document with all sections, see nature.com/documents/nr-reporting-summary-flat.pdf

Life sciences study design

All studies must disclose on these points even when the disclosure is negative.

Sample size	Sample sizes were not predetermined, but our sample sizes are similar or larger to those in previous studies (Toth et al., 2012; Donegan et al., 2020; Oliva et al., 2020; Boyle et al., 2024).
Data exclusions	Subjects with mistargeted viral injections and/or optic fibres were excluded from analyses. In addition, mice with fewer than 50 pyramidal neurons on day 1 of an experiment were excluded from the analyses, as well as mice which exhibited freezing for over 80% (240 s) of recall (<5% of total), which reduced interactions times and/or the amount of calcium events during social interactions to levels that were too low to quantify.
Replication	Experimental findings were reliably reproduced among all subjects in all experiments comprised of at least 3 cohorts.
Randomization	Mice were randomly assigned to a given group within the experimental conditions. The order of experimental trials was randomized. Stimulus mice and stimulus objects were randomly designated as the "CS+" or the "CS-" for individual experimental trials. The positions of the stimulus mice were chosen at random for recall, and swapped for experiments where further recall sessions followed.
Blinding	The experimenter was blinded to the experimental conditions.

Reporting for specific materials, systems and methods

We require information from authors about some types of materials, experimental systems and methods used in many studies. Here, indicate whether each material, system or method listed is relevant to your study. If you are not sure if a list item applies to your research, read the appropriate section before selecting a response.

Materials & experimental systems

n/a	Involved in the study
☐	☒ Antibodies
☒	☐ Eukaryotic cell lines
☒	☐ Palaeontology and archaeology
☐	☒ Animals and other organisms
☒	☐ Clinical data
☒	☐ Dual use research of concern

Methods

n/a	Involved in the study
☒	☐ ChIP-seq
☒	☐ Flow cytometry
☒	☐ MRI-based neuroimaging

Antibodies

Antibodies used

1) chicken anti-GFP (1:1000, AVES Labs, #GFP-1020, LOT# GFP3717982)
2) rabbit anti-RFP (1:1000, Rockland, #600-401-379, LOT# 48710)
3) mouse IgG2a anti-RGS14 (1:50, UC Davis/NIH NeuroMab Facility, #73-170, LOT# 472-1JU-12)
4) rabbit anti-PCP4 (1:400, Sigma-Aldrich; #HPA005792, LOT# 000047475)

Validation

Quality control information and relevant citations for antibodies used in this study are available at the following:
1) chicken anti-GFP: https://www.fishersci.com/shop/products/anti-chicken-gfp-0-4mg/NC9510598
2) rabbit anti-RFP: https://www.rockland.com/categories/primary-antibodies/rfp-antibody-pre-adsorbed-600-401-379/
3) mouse IgG2a anti-RGS14: https://neuromab.ucdavis.edu/datasheet/N133_21.pdf
4) rabbit anti-PCP4: https://www.sigmaaldrich.com/US/en/product/sigma/hpa005792

Animals and other research organisms

Policy information about studies involving animals; ARRIVE guidelines recommended for reporting animal research, and Sex and Gender in Research

Laboratory animals

8-14 week old male and female C57BL/6J, Amigo2-Cre and Avpr1b-Cre mice were used. Mice were maintained on a 12:12 light:dark cycle at 22°C and 40% humidity.

Wild animals

No wild animals were used.

Reporting on sex

Males and females were used for all experiments except only males were used for miniscope imaging experiments and experiments with CA2-silenced stimulus mice.

Field-collected samples

No field-collected samples were used.

Ethics oversight

All experimental procedures were approved by the Institutional Animal Care and Use Committee at Columbia University for the protocol AABJ7754.

Note that full information on the approval of the study protocol must also be provided in the manuscript.